Beach stability in Lake Macquarie entrance. December 1964.

Author:
Stone, D. M.

Publication details:
Report No. UNSW Water Research Laboratory Report No. 75

Publication Date:
1964

DOI:
https://doi.org/10.4225/53/5795a3aa4df27

THE UNIVERSITY OF NEW SOUTH WALES

WATER RESEARCH LABORATORY
Manly Vale, N.S.W., Australia

REPORT No. 75

Beach Stability in Lake Macquarie Entrance

by

D. M. Stone

https://doi.org/10.4225/53/5795a3aa4df27

DECEMBER, 1964

The University of New South Wales

WATER RESEARCH LABORATORY

BEACH STABILITY IN LAKE MACQUARIE ENTRANCE.

by

D. M. Stone

Report No. 75

Report submitted to Gutteridge, Haskins and Davey, Consulting Engineers,
December 1964.

Preface.

On behalf of Hooker-Rex Pty. Ltd., who are investigating the possibility of developing land along the southern shore of Lake Macquarie Entrance, Messrs. Gutteridge, Haskins and Davey, Consulting Engineers, commissioned the Water Research Laboratory through Unisearch Ltd. to undertake a model study to determine the nature of the wave action in the vicinity, and to test structures which might mitigate any adverse effects of such action.

The model was built between February and June 1964 and tested during July and August. The tests were conducted by Mr. K. K. Lai during the author's absence on leave. Analytic studies necessary for the proper design of the model and for the interpretation of model results proceeded concurrently with model building, and the analysis of the actual test results was made during September 1964.

Officers of both Hooker-Rex and Gutteridge, Haskins and Davey were kept informed of findings during the course of the study by the submission of progress reports covering the different phases of the work, and also by visiting the Laboratory to observe the model operating. Mr. Davey, for the Consultants, and Mr. Dalton, for Hooker-Rex, acted as liaison officers. The model was largely based on a hydrographic survey of 1954 kindly supplied by the Public Works Department of New South Wales.

H. R. Vallentine,
Assoc. Professor of Civil Engineering,
Officer-in-Charge.

Summary.

Model tests were undertaken to determine the nature of wave action along the southern shore of Lake Macquarie Entrance from the breakwater to Malt's Pt.

Analytic studies indicated that the waves most likely to result in erosive damage to the southern shore could be divided into two classes: first, short period waves from north east, and second, general ocean waves from east north-east to east. Since the latter group could reach greater heights and can also be expected to occur more frequently, the limited resources available were devoted to testing for this condition. A 7 ft. (prototype) ocean wave was used in the model, and wave heights in Salt's Bay were found to be about half the ocean wave height.

A marked littoral drift towards Malt's Pt. was found, extending from a point due south of the eastern end of the spur wall. The strongest littoral current, about 3 feet per second (prototype), occurred with a combination of 7 ft. ocean wave and tidal inflow of 26,500 c.f.s.; but a substantial current towards Malt's Pt. continued to be generated by all possible combinations of wave and tide. East of the spur wall, in the area immediately beyond the landward end of the southern breakwater, a slow counter-clockwise eddy was found with both ebb and flood of the tide.

It is recommended that a hydrographic survey be made, and the results compared with the 1954 survey to determine whether the littoral drift is being adequately supplied with sand so that the shoreline will remain stable. If erosion is occurring, preventive measures can be undertaken. Tests of various structures for mitigating against erosion indicate that the proposal to restore the western end of the existing spur and extend the spur a short distance to the east, raising the entire spur above mean high water, would be the most satisfactory solution.

Erosion just beyond the landward end of the southern breakwater is a separate problem, as it results from storm wave conditions which have not been tested on the model, probably the short period wave action from the north-east.

To reduce storm damage, dumping of large sized rock along the shore could be used, or a protecting spur could be built - again of large sized rock - running west from the landward end of the southern breakwater.

TABLE OF CONTENTS.

TABLE OF CONTENTS (cont'd.)

--- ------

LIST OF ILLUSTRATIONS

LIST OF ILLUSTRATIONS - (cont'd.)

LIST OF ILLUSTRATIONS , (cont'd)

APPENDIX 1:

1. Introduction

Lake Macquarie is one of the largest lakes in New South Wales. It flows to the sea about 10 miles south of Newcastle (Figure 1) and the entrance has been stabilised by breakwaters since about 1880. The breakwaters run E. N. E., and due east of the southern breakwater is an island which offers some protection against waves from the S. E. quadrant, so that it would appear that waves from some direction north of east are most likely to prove responsible for damage to the southern shoreline inside the breakwater. Tidal influence extends past the entrance and into the lake, and, though the rise and fall in the lake is small, the area subject to tidal influence is large enough to generate tidal currents of several knots through the entrance passage. These currents affect sand movements both intrinsically and because of the modifications they cause to the waves.

Figure 2 is a photograph of the eastern part of the entrance. About half-way between Swansea Bridge and the southern breakwater a spit of sand extends northerly from the southern shoreline - this is known as Malt's Pt. The area under study lies between Malt's Pt. and the southern breakwater, along the shore of Salt's Bay. East of Malt's Pt., running east-west, the freestanding remains of a wall that used to be joined to the southern training wall can be discerned. Some scattered rocks can be seen in Salt's Bay south of this so-called "spur wall", and in greater profusion in the south-eastern corner of the bay.

The entrance is quite shallow, with depths mostly less than one fathom except in the channel. Figure 3 shows soundings taken in 1954. Of special interest to this study is the high ground just inside the tip of the northern breakwater which continues southward as a bar across the entrance. The position of this bar can be located on the map by observation of the one-fathom contours. A depth of about 4 feet of water prevails. The position of the main tidal channel is also of interest - it can be seen hugging the northern shore until it reaches the breakwaters, where it swings towards the south avoiding the shallow water inside the tip of the northern breakwater.

The area modelled is virtually that shown in Figure 3. Reasons for this choice of model limits will be given in Section 3. 3. Before the model was built, however, the history of shoreline changes in the area was studied in some detail, as this can give valuable clues, not only on the shoreline processes at work, but also, and particularly is

this so for Lake Macquarie Entrance, on the chances of success for some structures that could help preserve the shore. A brief summary of historical facts considered pertinent is given in the next section, and model design and testing are discussed in the following sections.

2. Brief History of Erosion in Salt's Bay

Largely owing to the fact that the Public Works Department of the N. S. W. Government has been interested in the Lake Macquarie outlet, reliable historical data are available dating back to 1880, about the time when the breakwaters were built. However, a misinterpretation of high water and low water marks on an old map has led to the misconception prevalent in many circles that the present low water mark approximates that of 1880. Careful study of old maps reveals that the high water mark of 1880 has been misread by some investigators as low water, and this high water mark does in fact approximate the present shoreline. The 1880 low water mark was over 1000 feet farther out, making a wide zone subject to tidal influence. These data are shown on Figure 4, as well as data from maps of 1914, 1921 and 1929, and the survey of 1954 which gives the most recent complete coverage of the area.

Another popular misconception is that the spur wall shown on Figure 2 was at one time connected with the landward end of the southern breakwater. One reason for the perpetuation of this fallacy is obvious in Figure 2 - underwater rock can be seen extending from the landward end of the southern breakwater in line with the spur wall. However, this is a naturally occurring rock ledge, and its orientation relative to that of the spur wall is pure coincidence. The Public Works Department records indicate that the seaward end of the spur wall has never been substantially farther east than its present position.

The true sequence of events subsequent to the building of breakwaters and retaining walls can be ascertained by careful study of Figure 4. Eastward of the spur wall the low water level had receded by 1914 to a small extent from its 1879 location, and the 1914 line was then maintained practically unaltered until 1929. However, at some time between 1921 and 1929, two things happened towards the western end of the spur wall: a substantial westerly movement of a rather large quantity of material and a breakthrough in the spur wall itself. This breakthrough created a favourable climate for free circulation of water between Salt's Bay and the main water body around the freestanding remains of the spur wall. Between 1929 and 1954 substantial removal of material from Salt's Bay brought the general shoreline back to near

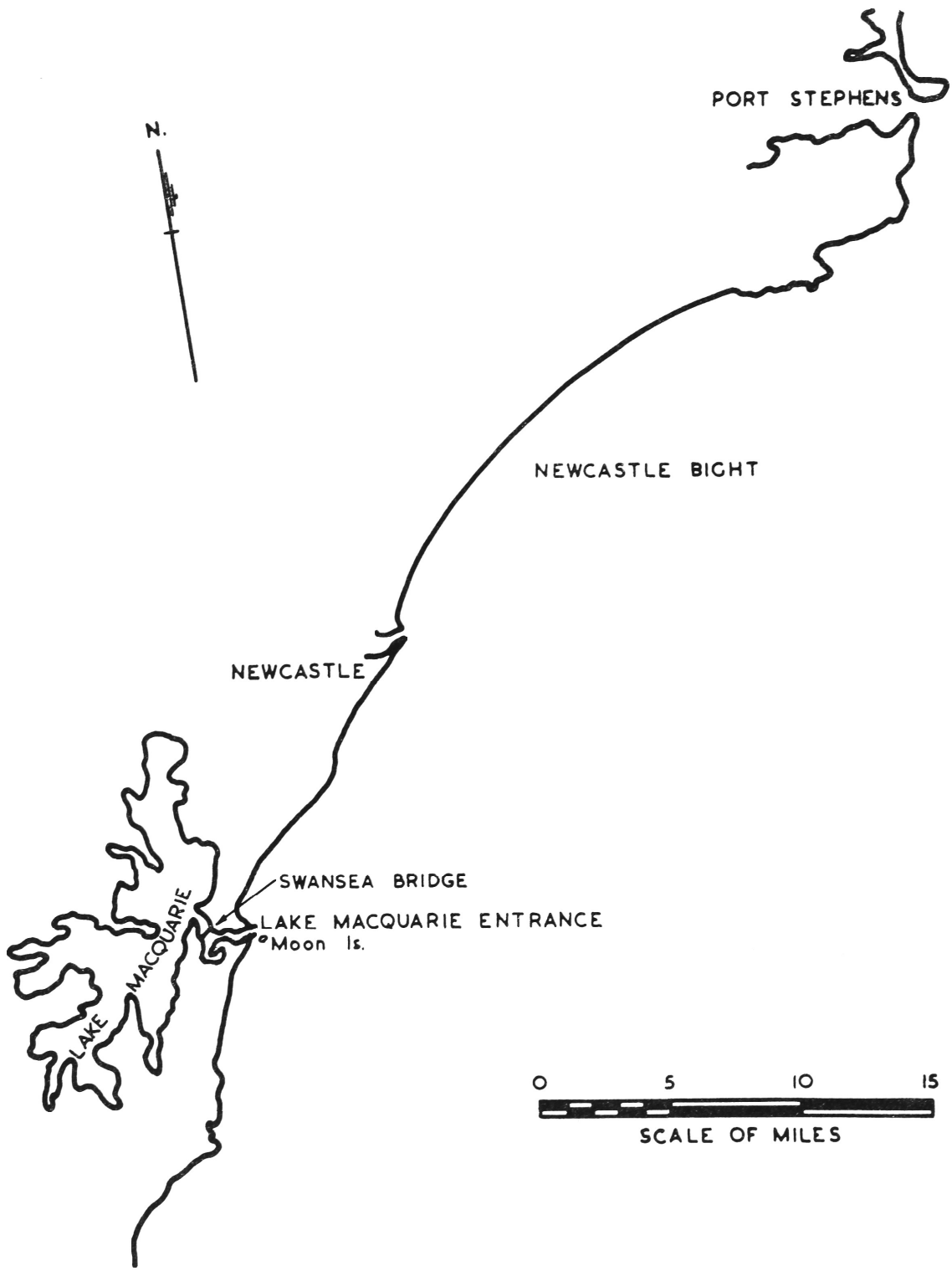

Figure 1: Location Plan

Figure 2: Aerial Photograph of Lake Macquarie Entrance from Breakwaters to Swansea Bridge. Photograph Adastra 1963.

Figure 3: Soundings in Lake Macquarie Entrance
P. W. D. Hydrographic Survey 1954.
Soundings in feet below I. S. L. W.

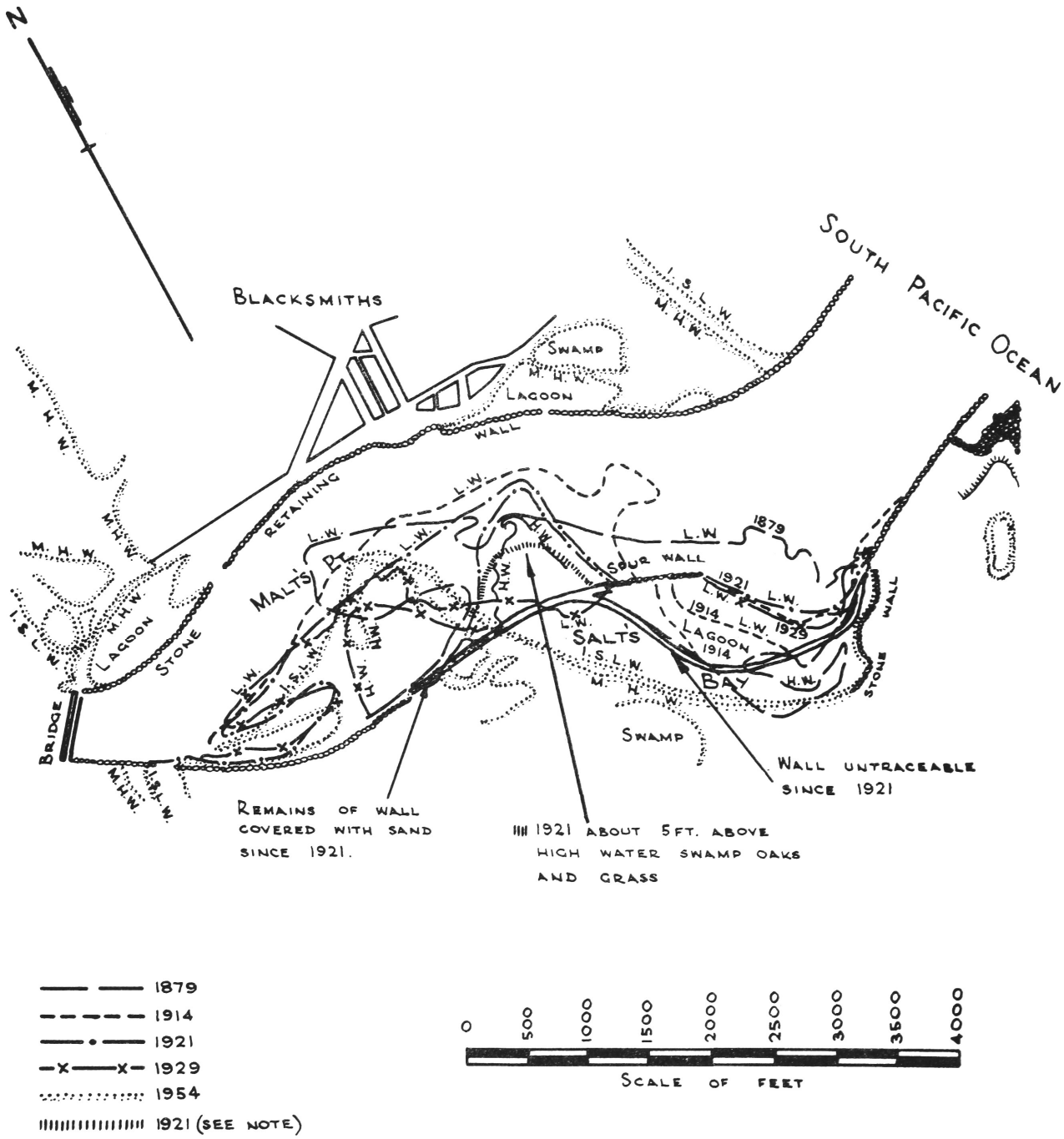

Figure 4 : Positions of Southern Shoreline of Lake Macquarie Entrance since 1879

its present position. The weight of evidence would lead one to believe that the major part of this recession occurred since 1942, when a shoreline position given on a military map indicates that the spur wall was still backed by land above sea level, the shore running from the eastern end of the spur wall in a curve halfway between the 1929 and 1954 low water marks to the southern breakwater. Local feeling is that heavy seas about 1945 caused considerable damage and subsequent periods of bad weather have worsened the situation. Though this has not been checked in exact detail it seems to fit in with the history as derived from recorded data.

In Figure 4 a stone wall can be seen extending in a southerly direction from the landward end of the southern breakwater. This was the position 1954. In the subsequent ten years, recession of this particular part of the shoreline has been considerable. Washaways have occurred at many places and the road leading to the Pilot Station on the cliff above the seaward end of the southern breakwater has been moved inland several times. It seems that the area originally surveyed for this road is now completely under water, though an exact shoreline survey has not been found.

References to settling, particularly as far as the spur wall is concenred, have been found in old newspapers. The fact that the top of the spur wall is now well below high tide level supports the settlement theory. The constructions in the area do not seem to have been maintained to any extent, particularly since about 1939, when coal traffic in the harbour eventually ceased and expenditure was no longer considered warranted. Removal of stone from some places by local residents has not helped towards keeping the walls in good repair. On the other hand it seems that rock has been dumped at various places from time to time by the local Shire Council to help maintain sea walls. Were improvements to be made to the port, the top of the breakwaters would be made to range from about RL. 12. 0 at the landward end to about RL. 17. 6 at the present seaward end, and the training walls would have a general level of about RL. 6. 5 with a gradation rising to RL. 12. 0 at the landward end of the breakwaters. From a survey undertaken during the course of this study for the purpose of finding levels for model construction, it is evident that present levels are considerably lower. The northern training wall ranges between RL. 2 and RL. 4 and the breakwaters nowhere reach a height above RL. 10.

Over the years, many breaks have occurred in the northern training wall through which water flows to lagoons behind the wall. These do not merit consideration as far as the model is concerned,

for their effect on wave action near the southern shoreline is not important.

3. Model Design

3.1 Data Sources

3.11 Soundings

Most of the data for construction of the model were taken from the 1954 P. W. D. Hydrographic Survey of the area. This is the most recent detailed survey available. As indicated in the previous section, some erosion has taken place in the area near the landward end of the southern breakwater in the intervening 10 years, but,without concomitant soundings, it was not considered wise to impose the new shoreline in this area on the model. The erosion extends for about one road width from the southern breakwater to the point where the shoreline turns from north-east to north-west.

3.12 Breakwaters

Breakwater levels were not given by the 1954 survey, and no data could be found giving the heights along the breakwaters at this time. The best that could be done was to make a breakwater survey at the present time and incorporate the results of this into the model on the assumption that levels in 1954 would not have been sufficiently different to vitiate model results. Figures 5, 6 and 7 relate to the breakwater survey.

3.13 Tide Levels

Part of the hydrographic plan of 1954 is presented in Figure 2. Another part, reproduced as Figure 8 of this report, shows the tidal gradient through the entrance. High tide at Malt's Pt. is given as 3 inches lower than ocean high tide. This difference would be represented by 1/16 inch on the model (vertical scale 1:50). The flow occasioned by such a small slope on the water surface (1/16 inch over about 30 feet) is too small compared with other factors to warrant the inclusion of expensive tide height reproducing equipment.

3.14 Tidal Currents

Tidal currents, on the other hand, are quite strong, and affect the patterns of flow in the entrance not only of themselves but also because of their influence on wave action. Preliminary testing in the model showed that changing the tidal discharge by a factor of 2 produced a

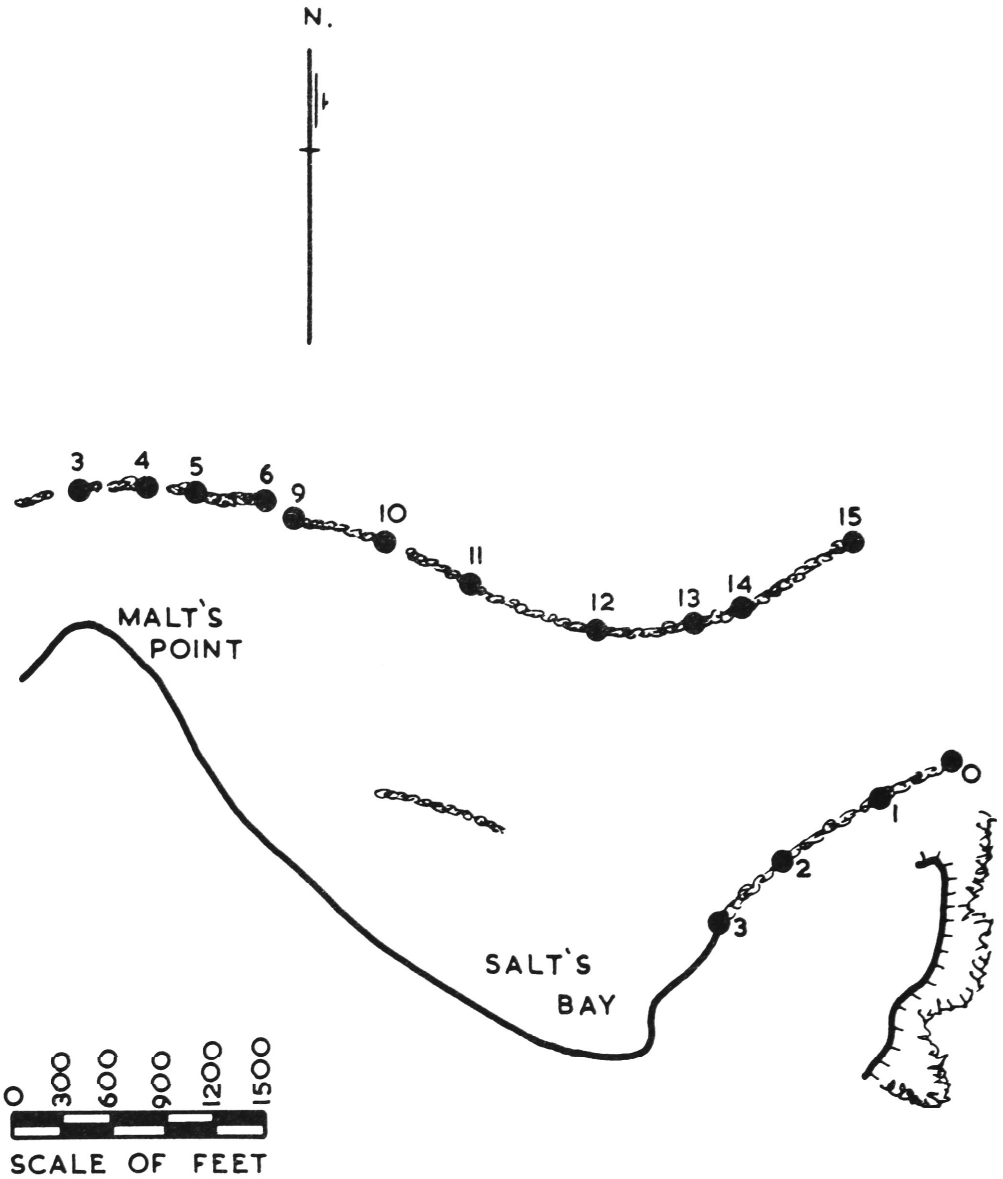

Figure 5: Plan of Survey Stations for Breakwater Levels

(SURVEY 14.5.64)

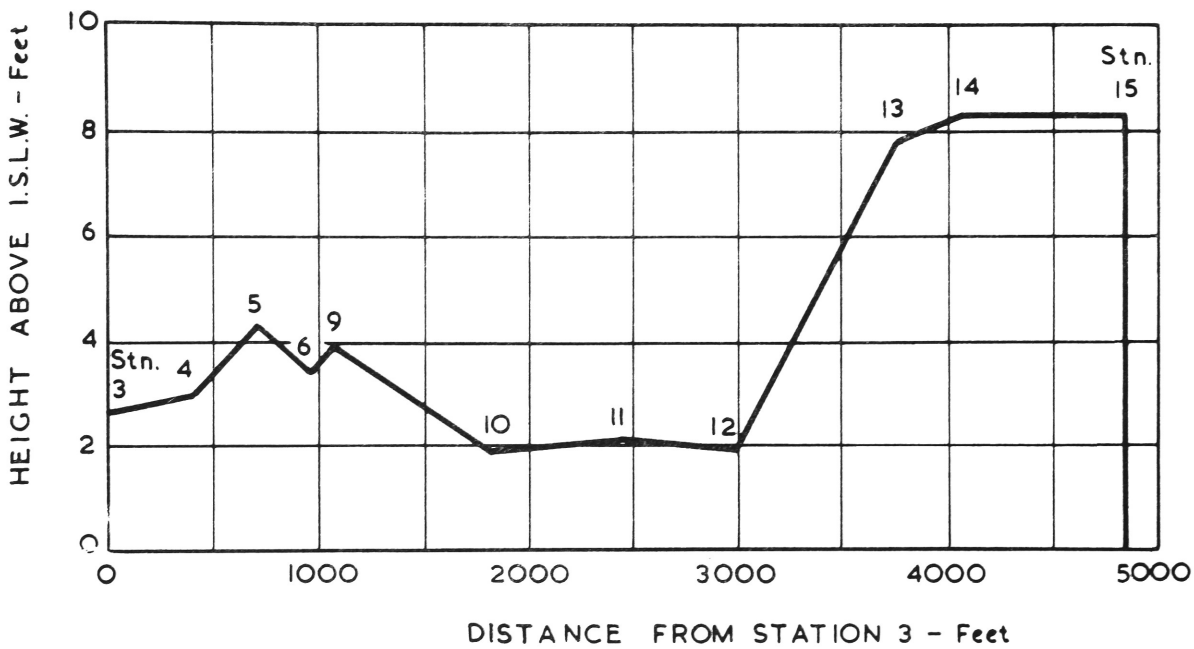

Figure 6: Longitudinal Profile of Breakwater - North Wall (Running Seaward)

(SURVEY 14.5.64)

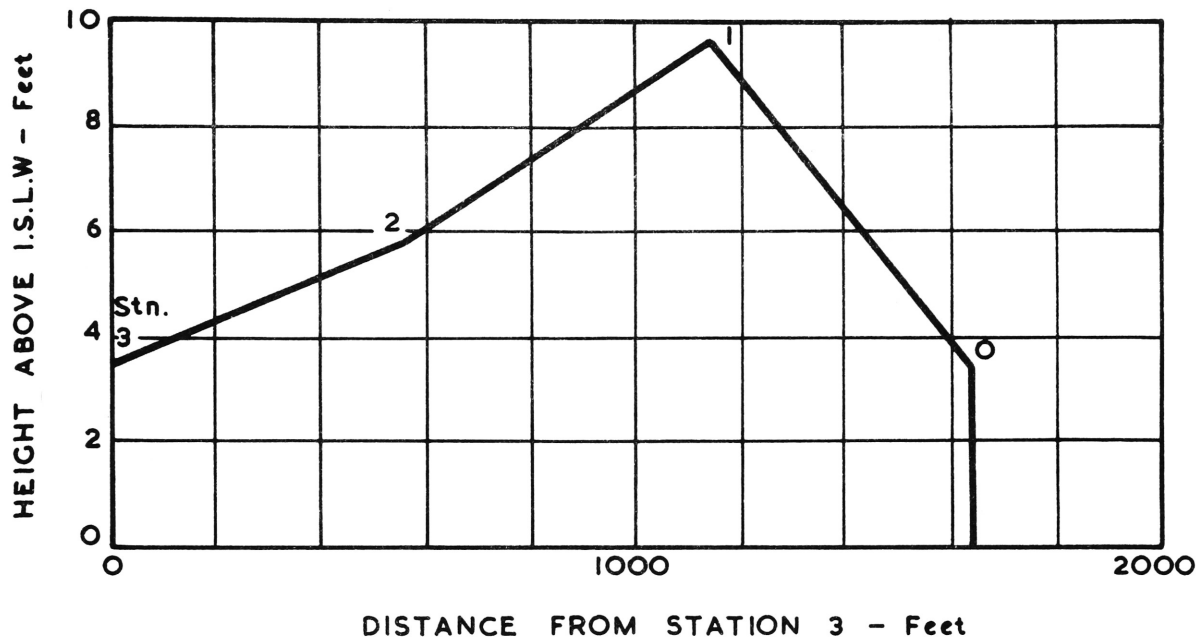

Figure 7: Longitudinal Profile of Breakwater - South Wall (Running Seaward)

(SURVEY 14.5.64)

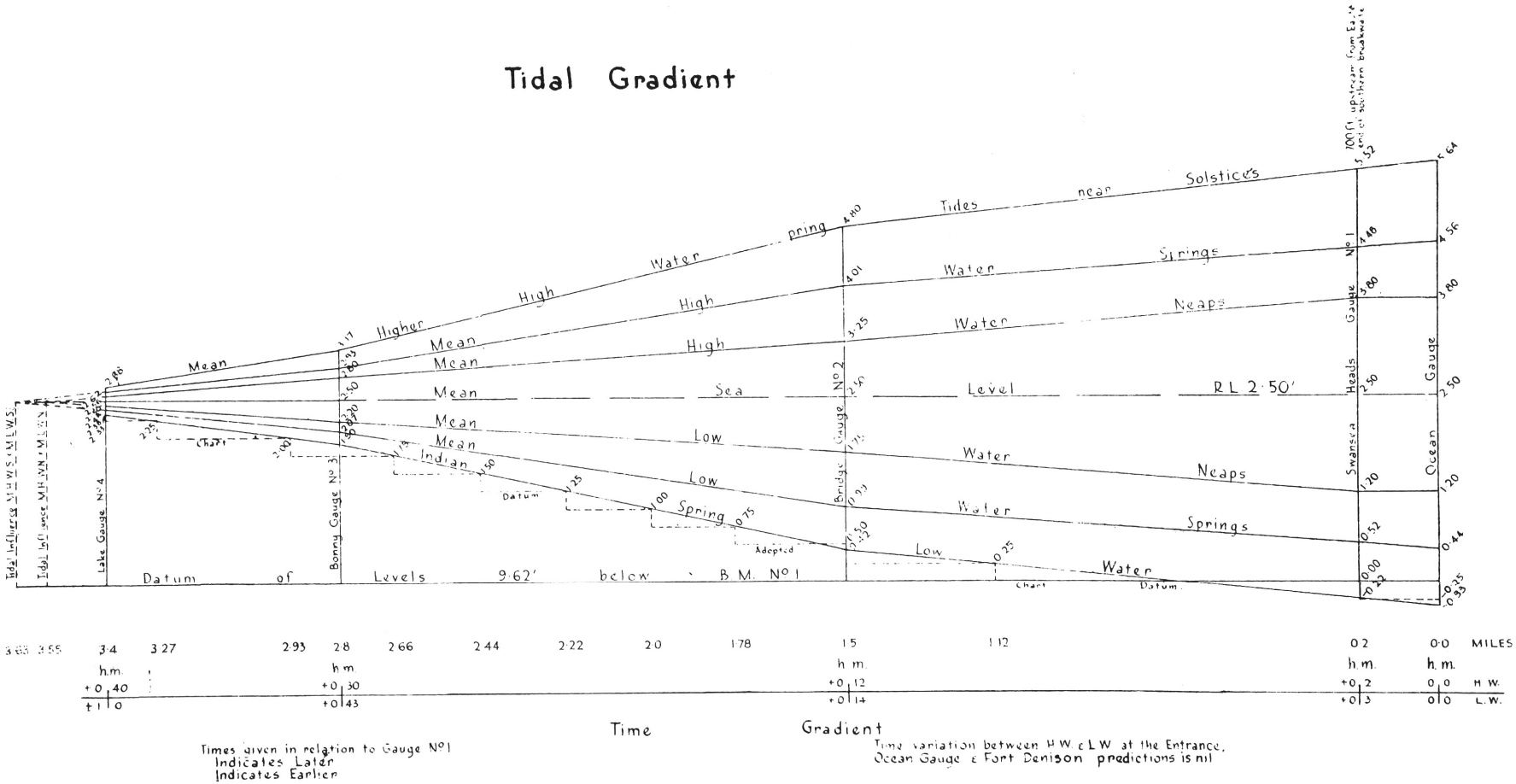

Figure 8: Tidal gradient through Lake Macquarie Entrance given by P.W.D. Hydrographic Survey 1954.

significant change in flow patterns. Pending the results of field measurements, the model tests had to be run with an estimated tidal discharge, and the method of obtaining a suitable figure is detailed in the following paragraphs.

Were sufficient information available, an estimate of the tidal discharge in the prototype could be made from the volume inflow and outflow based on tidal stages at various sections and a simple harmonic tide variation. However, the upstream limit of tidal influence is not precisely defined – it is only known that it is well past the entrance and into the lake. The tidal range within the lake is small, but the area of the lake subjected to tidal effects is large compared with the area of the entrance, and consequently the volume storage within the lake will be substantial. Hence estimates calculated from tidal inflow and outflow are liable to errors, and could be out by a factor of 2 or 3.

Under the circumstances, estimates based on tide velocities are apt to have just as high a degree of accuracy. We have two sets of data for such estimates. The Australia Pilot, Vol. III states "At half tide at Swansea wharves and in the channel past Pelican Islet, the tidal streams have a rate from 4 to 5 knots." Assuming that this applies to the main channel only and neglecting tidal discharge through other areas, we arrive at a discharge of 30,000 c.f.s. The second set of data for estimating tidal discharge is given with the P.W.D. Hydrographic Survey of 1954 which shows velocities in the main channel in the entrance between 1 and 2 knots. The discharge calculated for these velocities would be about 1/3 of that calculated from the Australia Pilot data. Since the tidal range for the P.W.D. data was not given, more reliance was placed on the higher figure given by the Australia Pilot, and the model was actually tested for tidal discharge of 26,500 c.f.s. prototype.

Subsequently, Hooker-Rex Pty. Ltd. undertook a programme of measurement of tidal currents. The data obtained are given in Appendix I. On the day when the measurements were taken, high tide in the ocean rose to 4.33 feet above I.S.L.W. and the tidal range was close to 3 feet. Maximum inflow velocities at the bridge section averaged about 2 feet per second. The sectional area under the bridge being roughly 8000 square feet at high tide, a tidal discharge of approximately 16,000 cubic feet per second is computed. Calculations for maximum outflow at low tide yield a similar estimate. Model tests were run for a high tide level at 5.2 feet above I.S.L.W. which can be seen from Figure 8 to represent a condition between mean high water springs and mean higher high water spring tides near solstices

and corresponds to a tidal range of 5.1 feet. If it is assumed that the effective surface area is independent of tidal range, a not unreasonable assumption for Lake Macquarie, then the tidal discharge is roughly proportional to the tidal range. Tidal discharge for 5.1 feet tidal range proportional to a discharge of 16,000 c.f.s. for 3 feet tidal range is 27,200 c.f.s. which is very close to the flow of 26,500 c.f.s. previously adopted for the model.

3.15 Waves

Data on maximum wave heights at sea are not required for this investigation because very large waves will not be able to reach Lake Macquarie Entrance without breaking on, or seaward of, the bar, thereby dissipating much of their energy. Worst erosion will result from the largest waves that can clear the bar without breaking, or with slightly larger waves which undergo partial breaking on the bar but still retain most of their energy. The first condition is simple to analyse and is sufficiently close to the second for a guide. From the solitary wave theory, which has been found to apply to conditions in or near the breaker zone (Sverdrup and Munk 1946, Ippen and Kulin 1955), we have the relation

$$y_b = 1.28\, H_b \qquad (1)$$

where

y_b = depth to still water level at breaking

H_b = wave height at breaking.

From Figure 3 we see that soundings across the bar show a limiting water depth of about 4 feet below I.S.L.W. Therefore at high tide a depth of 10 feet might be found. The wave height at breaking corresponding to this depth is given by (1) as just under 8 feet. The relation between the ocean wave height and the wave height at breaking will be discussed later. It is complicated by refraction and a subsequent section has been devoted to these questions. Suffice it here to say that, as will be shown later, waves from directions E.N.E. to E. can be generated with large enough height at sea to give a value of breaking wave height of 8 feet. This then is the criterion as far as wave height is concerned.

Wave period is another question. Many observations, some casual and some rather more sophisticated, have indicated that most waves off the New South Wales coast have periods lying in the range 6 seconds to 14 seconds with periods close to 10 seconds predominating. A wave period of 10 seconds has been chosen for the model tests as giving a fair representation.

Data on waves experienced within Lake Macquarie Entrance are lacking except for some casual observations by local residents that waves as high as 4 or 5 feet have been seen at high tide.

3. 2 Criteria for Waves for Model Tests

3. 21 North Easterly Waves

As can be seen from Figure 1, waves coming from the north-east towards Lake Macquarie blow over a limited fetch, since the headland south of Port Stephens prevents north-easterly ocean waves generated farther away from reaching the Lake Entrance even when refraction is taken into account. The maximum fetch being about 25 miles, and the average water depth about 90 feet, forecasting techniques for deep water can be used to give an idea of the waves at the Entrance for various wind speeds. Waves forecasted by the S. M. B. method (Bretschneider 1958) are given in Table 1.

TABLE 1.

WAVES AT LAKE MACQUARIE ENTRANCE CAUSED BY NORTH-EASTERLY WINDS.

(S. M. B. Deep water forecast for Fetch = 25 miles)

Wind Speed		Significant Wave Height*	Significant Wave Period*	Minimum Time Required to Generate such waves
Knots	Miles per hour	Feet	Seconds	Hours
50	58	14-1/2	8	2-1/4
40	46	9	6-1/2	2-1/2
30	34	6-1/2	6	3
20	23	4	5	3-1/2

* Significant wave height is defined as the mean of the heights of the highest one-third of the waves in a wave train, and is about 1.6 times

the average height (Wiegel 1961). The "maximum" wave used for designing structures against wave action is often taken as nearly twice as high as the significant wave. Significant wave period is the mean period associated with the significant wave height and is approximately equal to the mean period of all the waves in a train.

Since winds as high as 58 miles an hour have never been known to blow for as long as 2-1/4 hours continuously in this area, and it is dubious whether an average wind speed of 46 m.p.h. would be maintained for $2\frac{1}{2}$ hours, it can be taken that the period of the storm waves likely to be responsible for damage will not exceed about 6 seconds, as far as north-easterly weather is concerned. Figures 9 and 10 show the refraction of 6-second waves from the north-east as evidenced by the bending of the "wave rays" or orthogonals to the crests (Arthur, Munk and Isaacs, 1952). The rays are plotted as far as the 7 fathom contour on Figure 9; at this depth, the turning has been about 3^{o} and the spacing between rays A and B has increased to about $1\frac{1}{2}$ times the spacing in effectively deep water. Since wave height ratio is inversely proportional to the square root of spacing ratio for any pair of rays, it is seen that the wave energy has spread over a greater crest length so that the wave height at 7 fathoms is only about 80 pc. of the wave height at sea. Figure 10 shows that the spacing of the rays increases by about 30 pc. between the 7fathom contour and the breakwaters, and there is little further turning. The wave height at the breakwaters is therefore 85 pc. of that at 7 fathoms, and consequently 85 pc x 80 pc. = 70 pc. of the deep water wave height. The general conclusion is that north-easterly waves will penetrate the entrance with a direction very close to their original direction and with their height reduced to about 70 pc. of their deep water height, as far as refraction is concerned. It will be noted that the contours plotted on Figure 10 are for depths at mean high water since this is regarded as the condition for maximum wave penetration and erosion damage. At low water, waves are more likely to break over the bar just inside the entrance of the breakwaters and thereby dissipate much of their energy. Also,for the smaller water depth, refraction will be greater and consequently the wave heights smaller. Subsequent reforming of waves within the entrance after a break on the bar is not likely to create conditions bad enough to be regarded as design criteria.

For the variation of wave parameters in shoaling water the work of Mason (1951) and the U.S. Navy Hydrographic Office (1944) is used. Figure 11 shows the effects of decreasing water depth on a wave where there is no refraction. From the relation for sinusoidal waves:

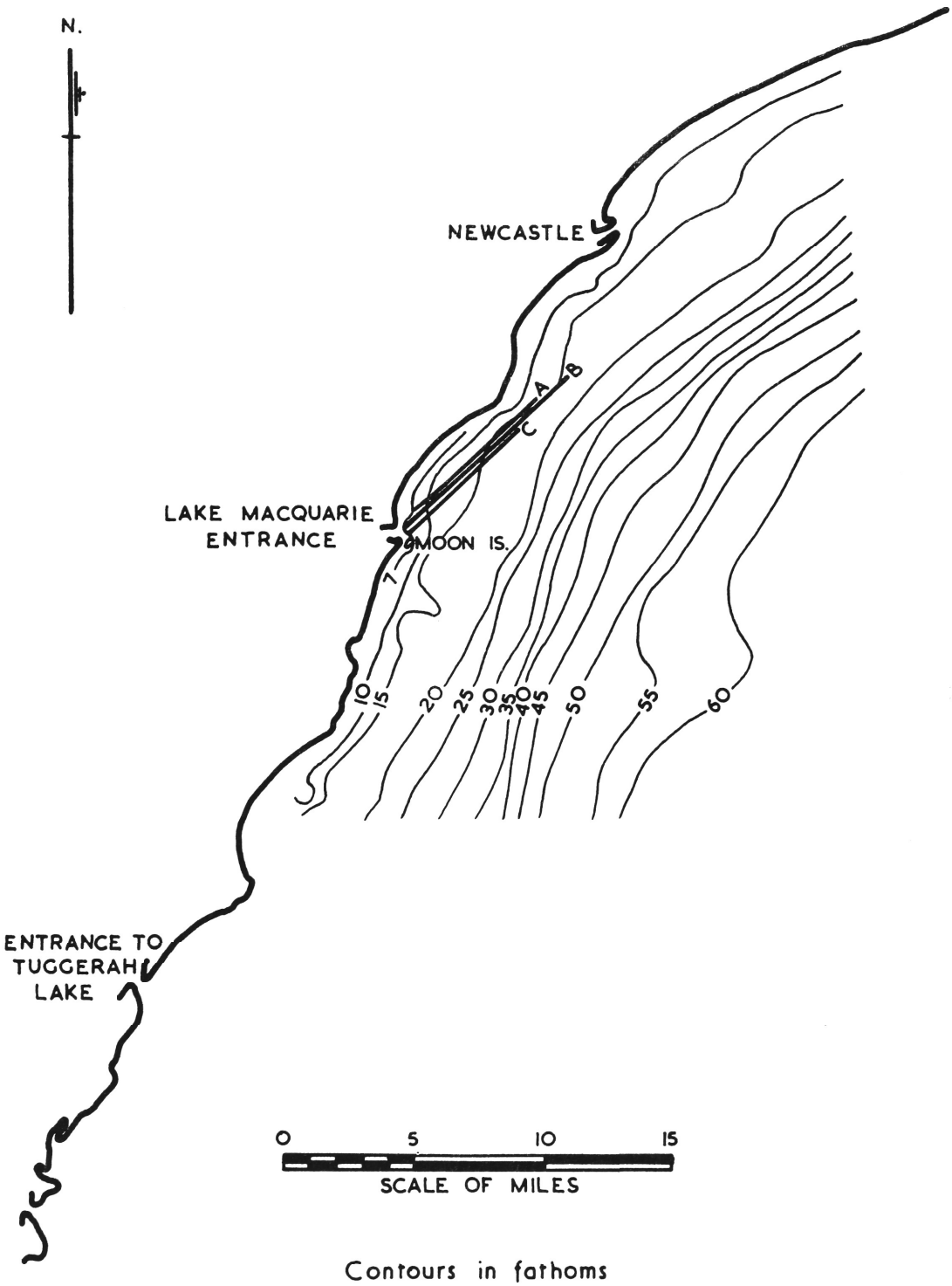

Figure 9 : Refraction Diagram for 6 second Waves from North East - Deep water to 7 fathoms

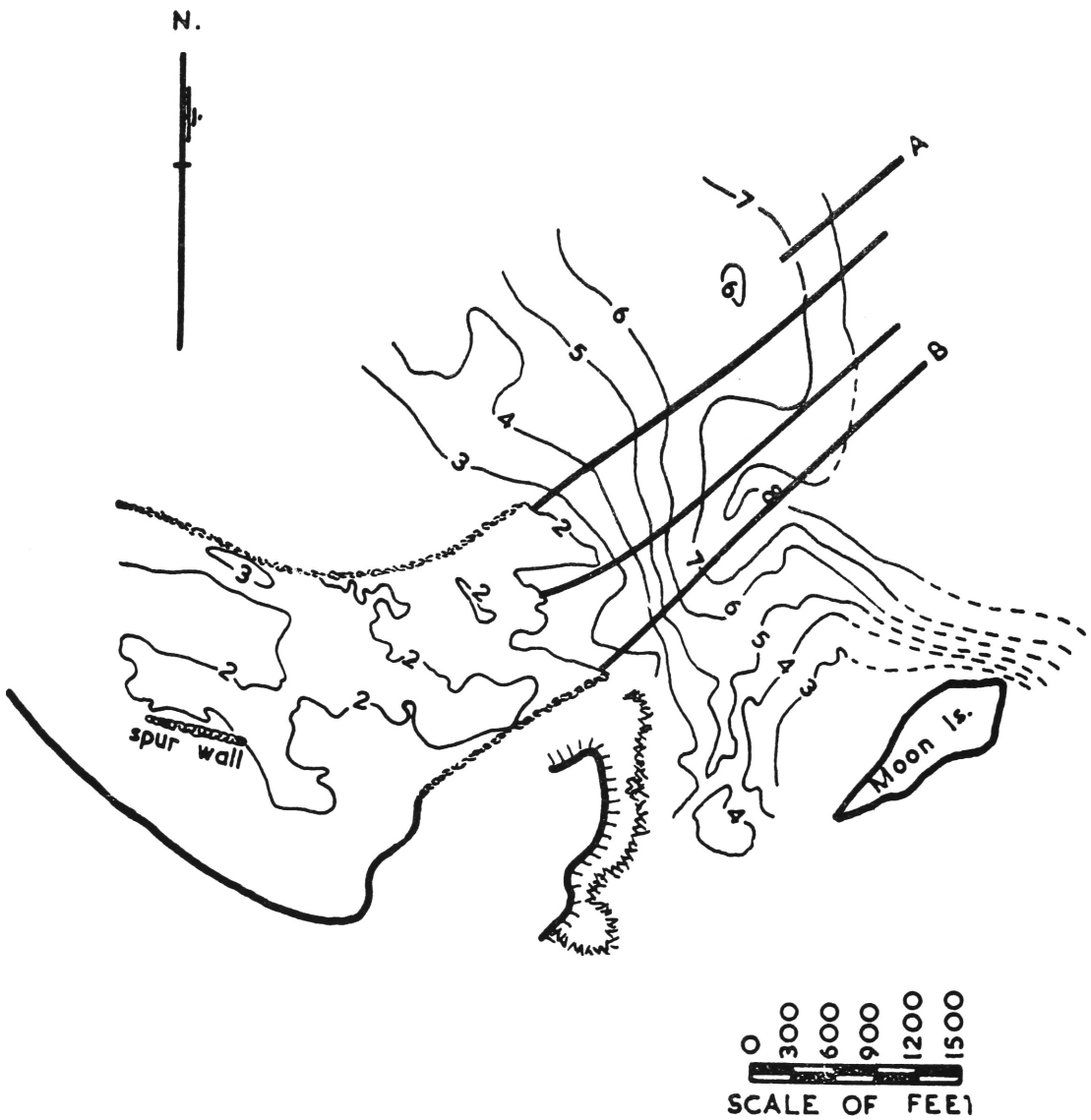

Contours in fathoms at mean high water

Figure 10: Refraction Diagram for 6 second Waves from North East

7 fathoms to 2 fathoms

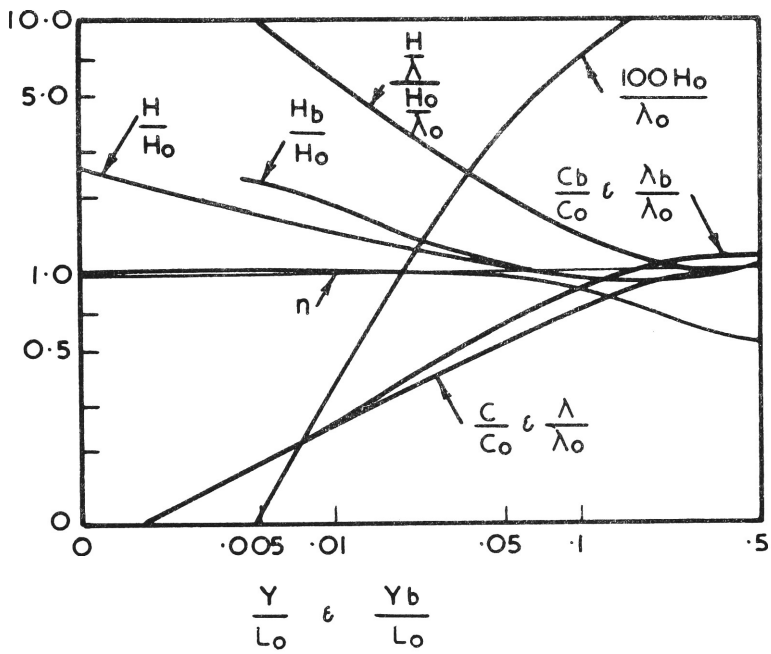

Figure 11: Shoaling Effects on Waves

after U.S Navy Hydrographic Office: "Breakers & Surf - Principles in Forecasting." Nov. 1944.

$$\lambda_o = \frac{g}{2} \frac{T_o^2}{\pi} \qquad (2)$$

where λ_o = wave length in deep water

g = gravitational acceleration

T_o = wave period in deep water

(U.S. Beach Erosion Board, 1942), we find the λ_o for six second waves to be 184 feet. Assuming a depth over the bar of 10 feet at high water we find from (1) H_b = 7.8 ft. From Figure 11 with $\frac{y_b}{L_o} = \frac{10}{184} = 0.055$ we find $\frac{Hb}{H_o} = 1$ and therefore H_o for no refraction = 7.8 feet. Taking refraction into account we see that ocean waves from the north east with an ocean wave height of 11 feet and a period of 6 seconds would just break on the bar. From Table 1 it can be seen that these waves are higher than any likely to be generated with a 6 second period. It is therefore obvious that the waves likely to cause damage which lie in the range between 9 feet $6\frac{1}{2}$ seconds and $6\frac{1}{2}$ feet 6 seconds (corresponding to 40 knot wind blowing for $2\frac{1}{2}$ hours and 30 knot wind blowing for 3 hours, respectively) will continue over the bar at high water without breaking.

3.22 Waves from East-North-East through East to South

Waves from directions east-north-east through east to south blow over an unlimited fetch and have been known to achieve significant wave heights of 30 feet off the New South Wales coast. Wave periods generally in the range 6 seconds to 16 seconds are found, the shorter periods being associated with locally generated storm waves and the longer periods with swell from distant storms. A wave period of 10 seconds is frequently used as a representative figure, and refraction diagrams have been drawn for this period for waves from E.N.E., E., S.E. and S. Waves of higher period will suffer more refraction and those of lower period less. Table 2 will give some idea of the meteorological conditions that can be associated with a 10 second period wave, as far as a locally generated sea is concerned. For swell, the wave period increases while the height decreases as the swell travels through the decay area, and 10 second waves at shore would result from storms generating a wave of smaller period at sea.

TABLE 2.

CONDITIONS ASSOCIATED WITH 10 SECOND STORM WAVES.

(S. M. B. Forecast)

Wind Speed		Significant Wave Height	Minimum Fetch required to generate such waves.	Minimum time required to generate such waves.
Knots	Miles per Hour	Feet	Miles	Hours
50	58	18	70	5
40	46	16	110	8
30	34	13	180	14
20	23	9	550	43

From equations (1) and (2) and Figure 11 we see that, for the condition of negligible refraction effect on wave height, λ_o = 512 ft., $\frac{y_b}{\lambda_o}$ (for y_b = 10 feet) = 0.195, $\frac{H_b}{H_o}$ = 0.9 and therefore, since H_b = 7.8 feet, H_o = 8.7 feet. This corresponds to a wind of about 20 knots blowing for 43 hours over a fetch of 550 miles, a not unlikely occurrence. Refraction effects make some alteration to these figures, as shown in subsequent sections. As far as swell is concerned, a study of wave forecasting and decay curves reveals that waves leaving a generating area more than about 100 miles away would generally have periods in excess of 10 seconds if they were to have a wave height after passing through the decay area as great as 8.7 feet.

3.23 Waves from East-North-East

Figures 12 and 13 show that 10 second waves from E.N.E. turn through between 5^o and 10^o by the time they reach the breakwaters and that the spacing of the rays remains quite similar to the deep water value. The height of ocean wave such that penetration within the entrance of maximum destructive energy takes place will therefore be about the value previously computed, i.e. 8.7 feet.

3.24 Waves from East

Figures 14 and 15 show that waves from the east turn slightly towards the north by the time they reach the 7 fathom contour, but are

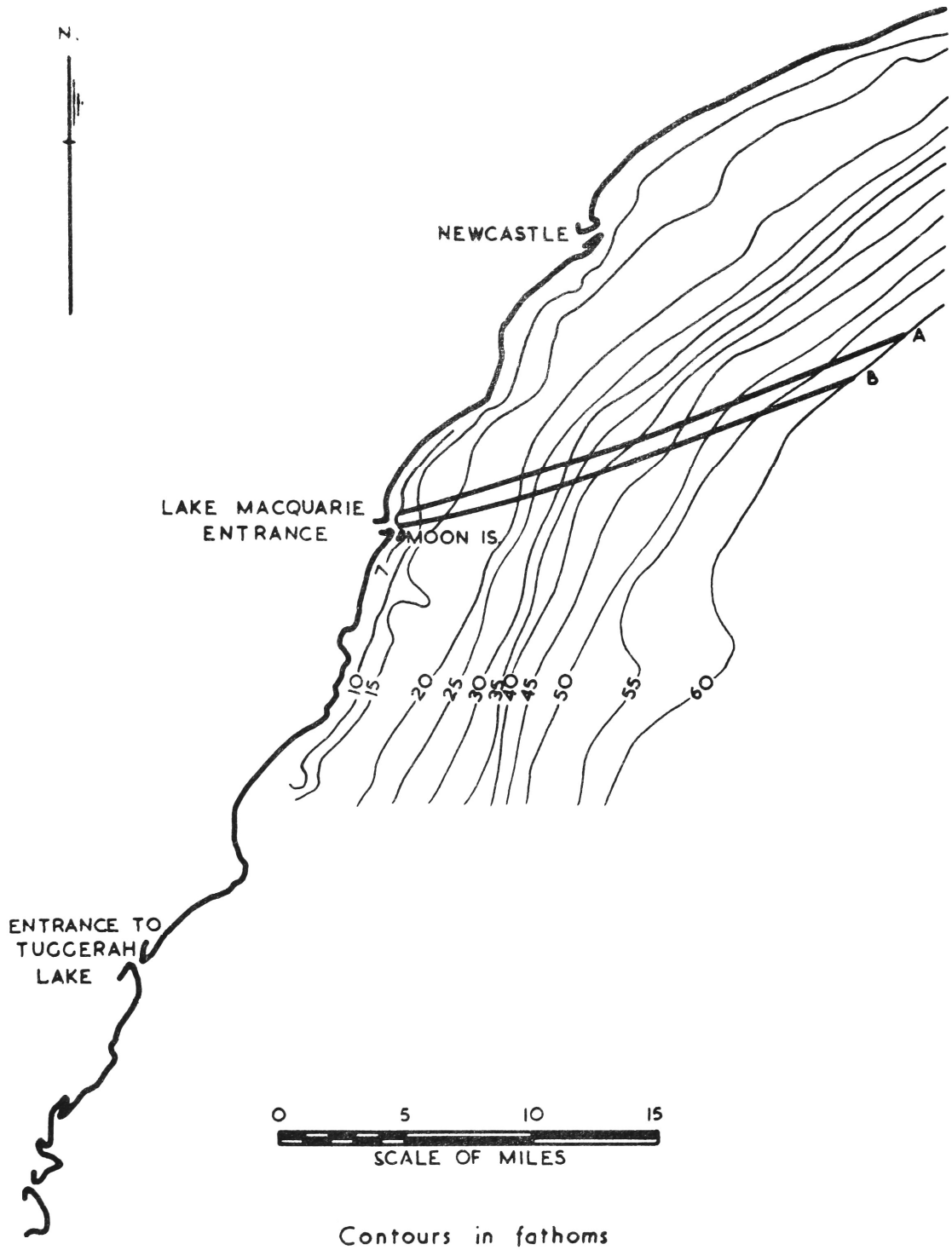

Figure 12: Refraction Diagram for 10 second Waves from East North East - Deep water to 7 fathoms

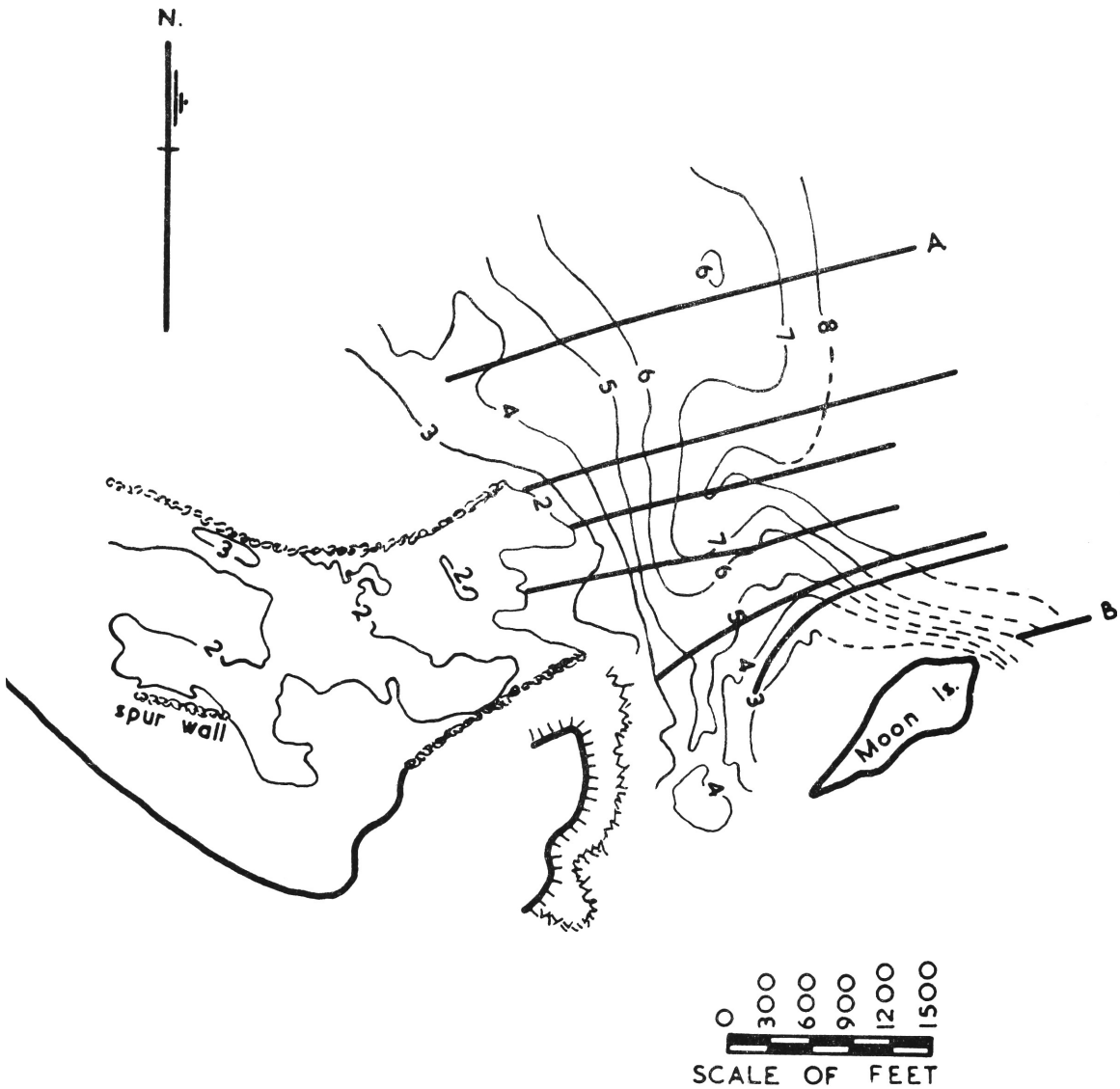

Contours in fathoms at mean high water

Figure 13: Refraction Diagram for 10 second Waves from East North East

7 fathoms to 2 fathoms

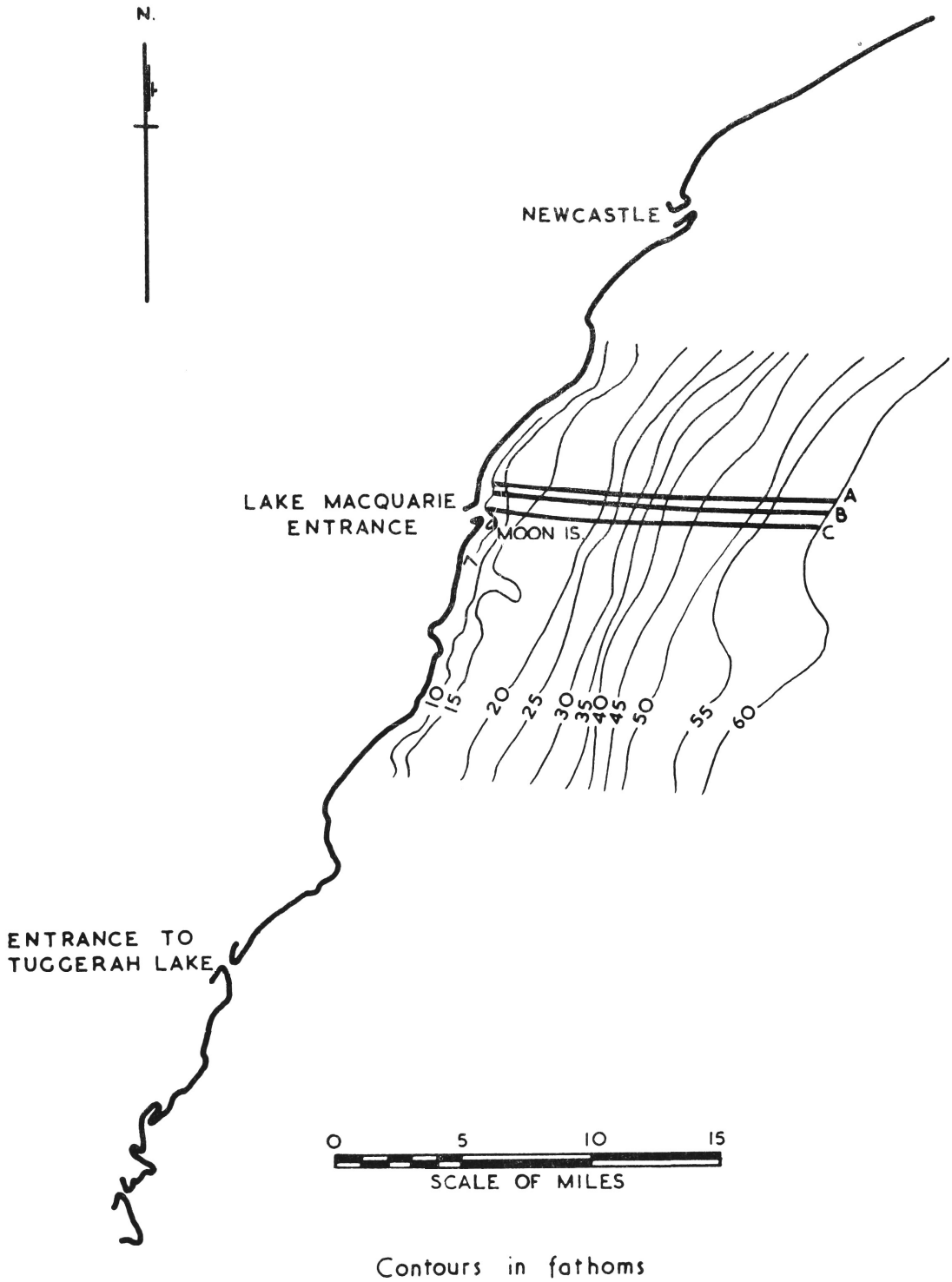

Figure 14: Refraction Diagram for 10 second Waves from East - Deep water to 7 fathoms

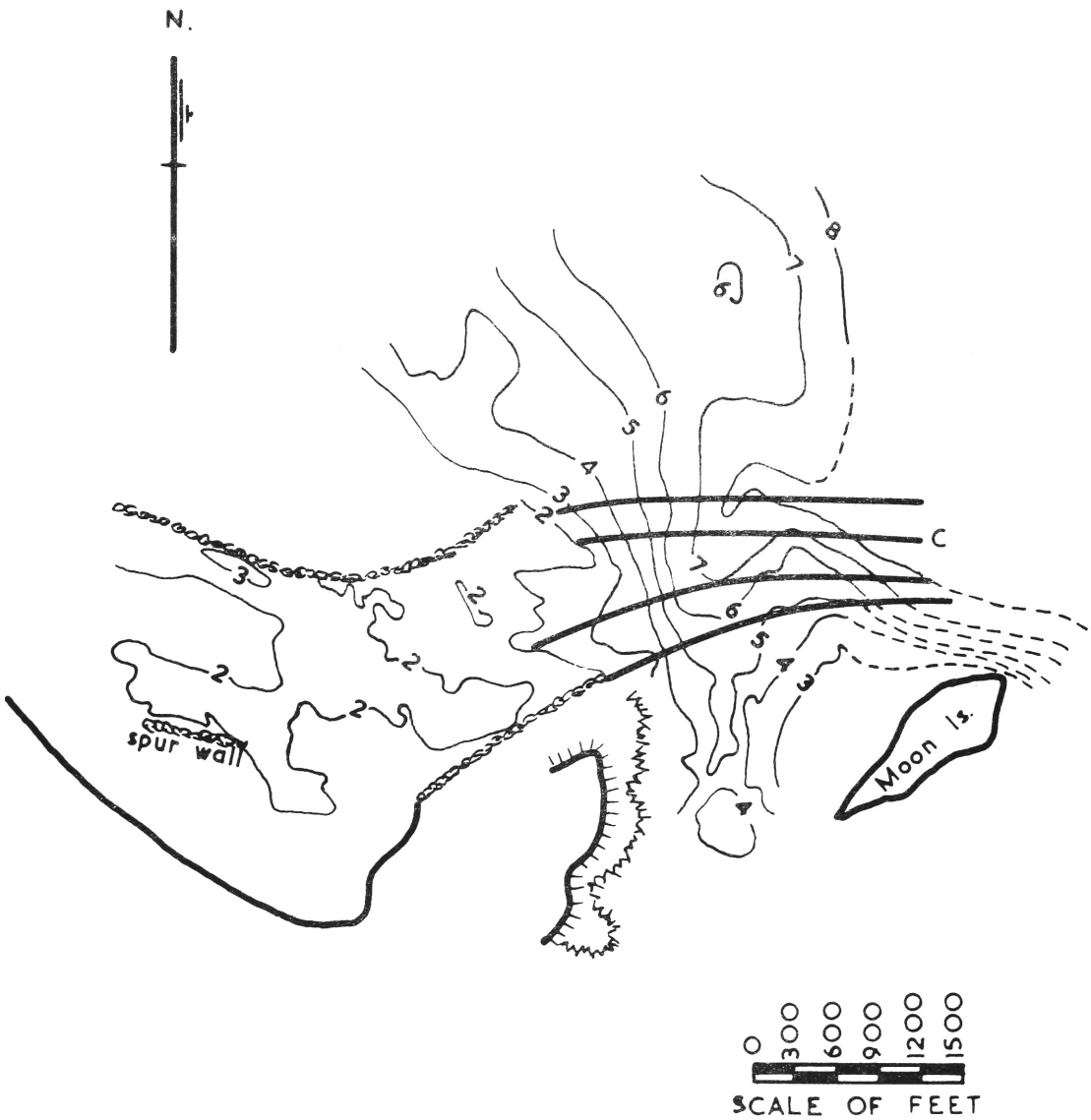

Contours in fathoms at mean high water

Figure 15: Refraction Diagram for 10 second Waves from East

7 fathoms to 2 fathoms

bent farther back by subsequent refraction so that the directions of the rays at the breakwaters are between 5^{o} and 20^{o} north of east.

Wave height is reduced to 80 pc. of the deep water value so that a 9.8 foot 10 second wave is the design criterion. Such a wave would require a wind of about 20 knots to blow for 43 hours over 550 miles for generation, as can be seen from Table 2.

Thus waves from the E.N.E. and E. should act with great destructive force on the southern shoreline, and when a storm is in progress with waves from between E.N.E. and E. all the energy will be concentrated in the entrance. The wave paddle in the model has been oriented to suit the direction of these waves at the 4 fathom contour, i.e. the paddle is perpendicular to a line running 15^{o} north of east.

3.25 Waves from South-East

Figure 16 shows wave refraction for waves from S.E. as far as the 7 fathom contour. These waves suffer little refraction and are largely prevented from penetrating the entrance by Moon Island, as can be seen by observing the position of the island in Figure 9. Some diffraction may occur around the island, and a small amount of wave energy could enter from this cause, but as far as destructive action on the southern shore is concerned, this can be neglected.

3.26 Waves from South

Figure 17 shows that waves from south are bent by refraction through 20^{o} so that they reach the 7 fathom contour with direction 20^{o} east of south. Figure 18 shows that some of these waves will travel through the channel between Moon Island and the mainland. Some of these waves will be refracted into the entrance and some will strike the northern breakwater, but the amount of energy transmitted in this way will be small, as can be seen from the divergence of the wave rays. On average, the spacing of the wave rays at the entrance to the breakwaters is nine times the deep water spacing so that wave heights will be reduced in the ratio 1:3. Since the channel between Moon Island and the mainland has a depth at high water somewhat less than 24 feet no ocean wave greater than about 18 feet could travel up the channel without breaking. An 18 foot wave would be reduced by the time it reached the breakwaters, to about 6 feet because of refraction, so southerly waves running up the channel are hardly likely to present a critical case for erosion on the shore of Salt's Bay.

3.27 Diffraction of Waves

For this particular area, wave diffraction would be most pronounced for waves from south-east and south. In order to penetrate the entrance, waves from the south-east would indeed have to diffract around Moon Island. Since diffraction is important only for near vertical breakwaters and very steeply shelving rock cliffs, it can be seen that the amount of energy transmitted by this means would not create a condition promoting destructive erosion in the entrance. Since only those southerly waves that travel up the passage between Moon Island and the mainland can affect conditions in the entrance, the wave energy arising from the diffraction of such waves around the tip of the southern breakwater would not be great. Thus, it does not seem necessary to produce diffraction patterns for either south-easterly or southerly waves since the energy involved is so slight.

3.28 Choice of Waves for Model Tests

The preceding sections have shown that the waves likely to cause the greatest concern along the southern shore of Lake Macquarie Entrance can be divided for model considerations into two classes. First there are the short period (6 second) locally generated waves from north-east which may attain an ocean wave height between $6\frac{1}{2}$ feet and 9 feet, the height being reduced by refraction to 70 pc. of the ocean wave height, or between 4.5 and 6.3 feet, by the time the waves reach the breakwaters. Secondly, there are waves of a range of periods from east-north-east to east which may attain great heights, but of which those higher than 7.8 feet will break and so dissipate some of their energy before reaching the entrance. For waves from these directions, a height of 7.8 feet and period of 10 seconds can be taken as representative.

Logically, model tests should be made for both of these classes of wave. However, this would entail either the construction of a movable wave generator or the relocation of the fixed generator between the two sets of tests. In the time available it was possible to test for only one of the two conditions, and the tests were made for the second condition, representing waves from east-north-east or east. Reasons for this choice are:-

(1) As can be seen above, higher waves can enter from this quarter.

(2) The longer period waves are subject to greater refraction effects

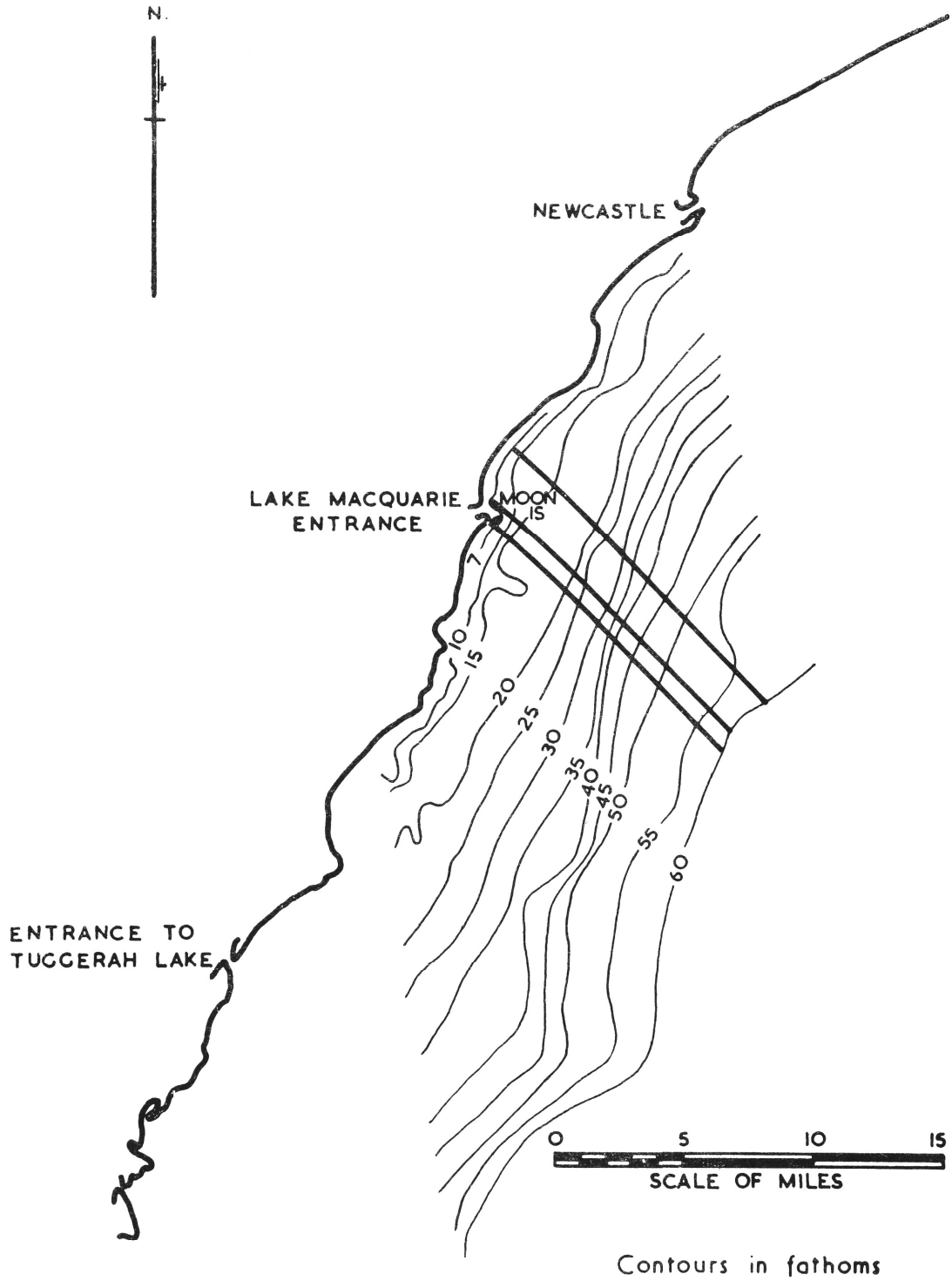

Figure 16: Refraction Diagram for 10 second Waves from South East - Deep water to 7 fathoms

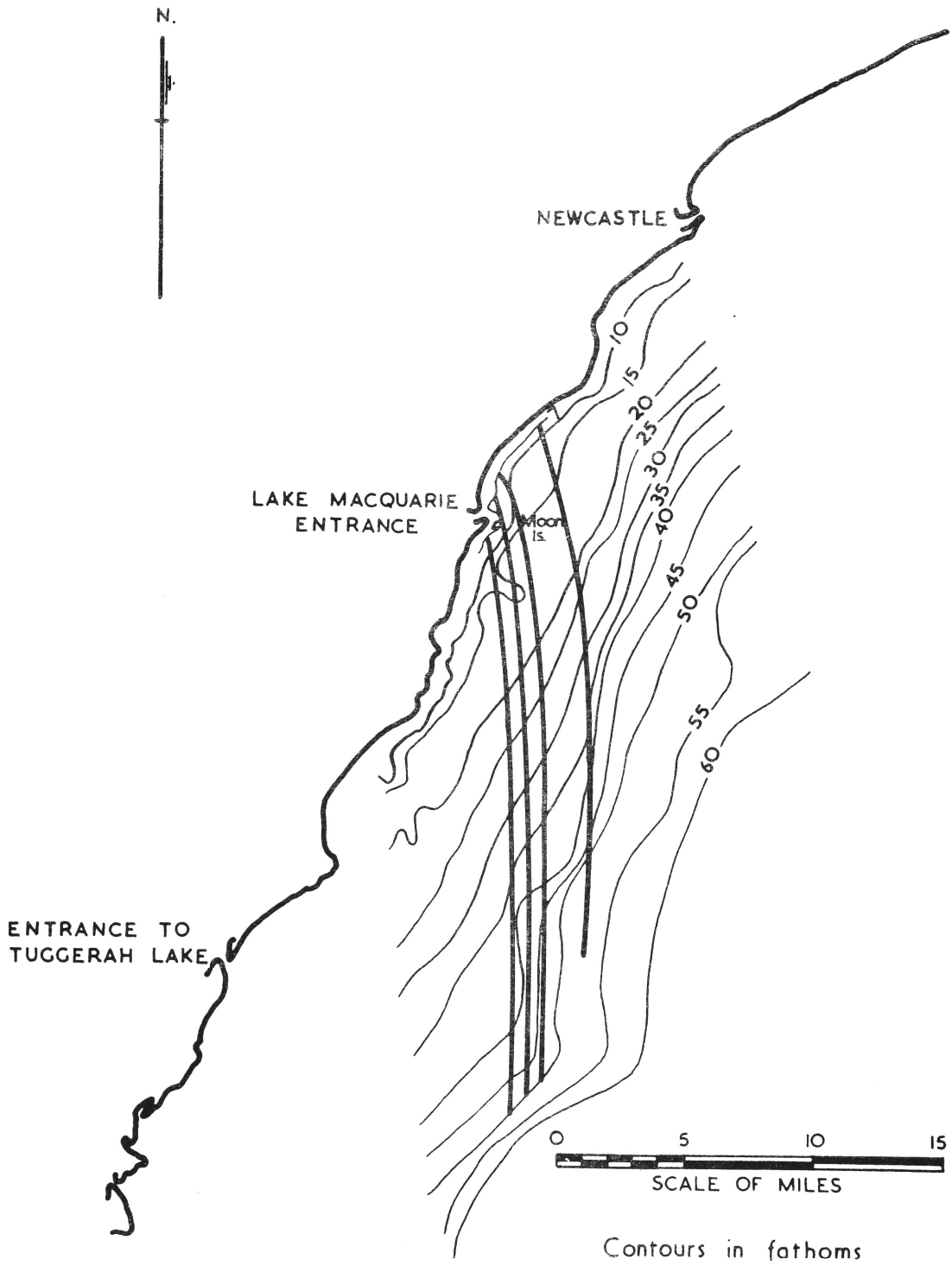

Figure 17: Refraction Diagram for 10 second Waves from South – Deep water to 7 fathoms

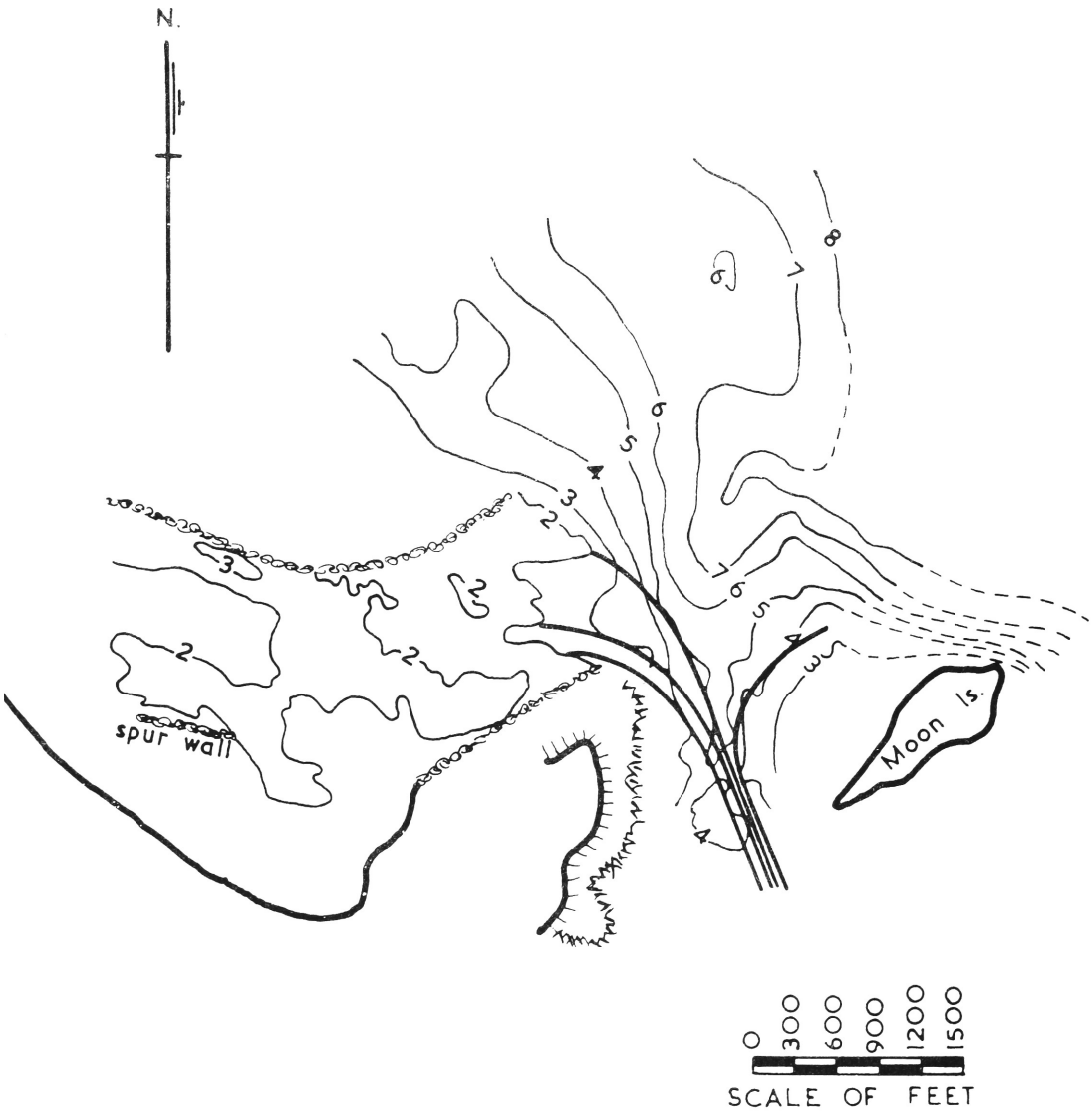

Contours in fathoms at mean high water

Figure 18: Refraction Diagram for 10 second Waves from South

7 fathoms to 2 fathoms

within the entrance, and are therefore less amenable to analysis.

(3) Wave action from the east is stronger and more frequent in this area than wave action from the north-east*. Furthermore the condition covers waves from east-north-east as well as east, whereas the alternative covers waves from north-east only, and the chosen condition therefore represents a greater sector of the compass.

3.3 Model details

3.31 Model limits

With the distribution of tidal flow across the entrance unknown when the model was built, it was necessary to extend the model upstream to a point where direction and distribution of flow could reasonably be assumed and properly reproduced. Observation of figures 2 and 3 will show that at Malt's Pt a suitable channel section exists, and this was chosen as the upstream limit.. The ocean side model limits were chosen far enough from the breakwaters to allow waves generated by a simple hinged paddle to attain their proper configuration before reaching the breakwaters. Figure 19 shows the area covered by the model.

3.32 Model scales

To fit the model into a reasonable space, in this case an existing wave basin 45 feet by 30 feet, a horizontal scale of 1:150 was the largest that could be chosen concomitant with desirable model limits as specified above. A vertical scale of 1:50 was chosen as a compromise between accuracy of measurement of water depth and wave heights and minimal distortion. With wave heights scaled to the vertical ratio, a 4 foot prototype wave is thus represented on the model by a one inch wave, and this is substantially above the limit between gravity waves and surface tension ripples which occurs at a wave height of about 1/4 inch, so that surface tension effects should not be too important. At the same time the distortion is kept down to a 1:3 ratio; at this level many of the deleterious effects of distortion in wave models will be ameliorated, while analytic studies can make allowance for some effects in scaling up from model to prototype. There are some factors which will not be correctly reproduced on the model and these will be discussed later in this section. For this particular model, these factors are not considered to play a dominant role in the problem.

* This result comes from an analysis, not yet published, of 5 years of records by forecasting techniques.

For a free surface model, the velocity scale is given by the Froude similarity criterion as

$$\frac{V_p}{\sqrt{gd_p}} = \frac{V_m}{\sqrt{gd_m}} \qquad (3)$$

where V = a velocity
d = a vertical dimension
g = gravitational acceleration
p = a subscript referring to prototype values
and m = a subscript referring to model values

Expressed in terms of scale ratios (3) becomes

$$V_r = \sqrt{d_r} \qquad (4)$$

where r = a subscript denoting the ratio of a prototype to a model quantity (otherwise referred to as scale)

With d_r for this model equal to 50

$$V_r = \sqrt{50}$$

$$= 7.07$$

The discharge scale for the model is given by

$$Q_r = A_r V_r$$

$$= L_r \; d_r \sqrt{d_r}$$

$$= 150 \times 50 \times 7.07$$

$$= 53,000$$

The tidal discharge used for the model was 26,500 c.f.s. prototype and the discharge through the model was therefore 0.5 c.f.s.

Since tidal currents are scaled to Froude similarity, it would be expedient to scale the wave velocities by the same law. This is sometimes referred to as "distorted" wave scaling as distinct from "undistorted"

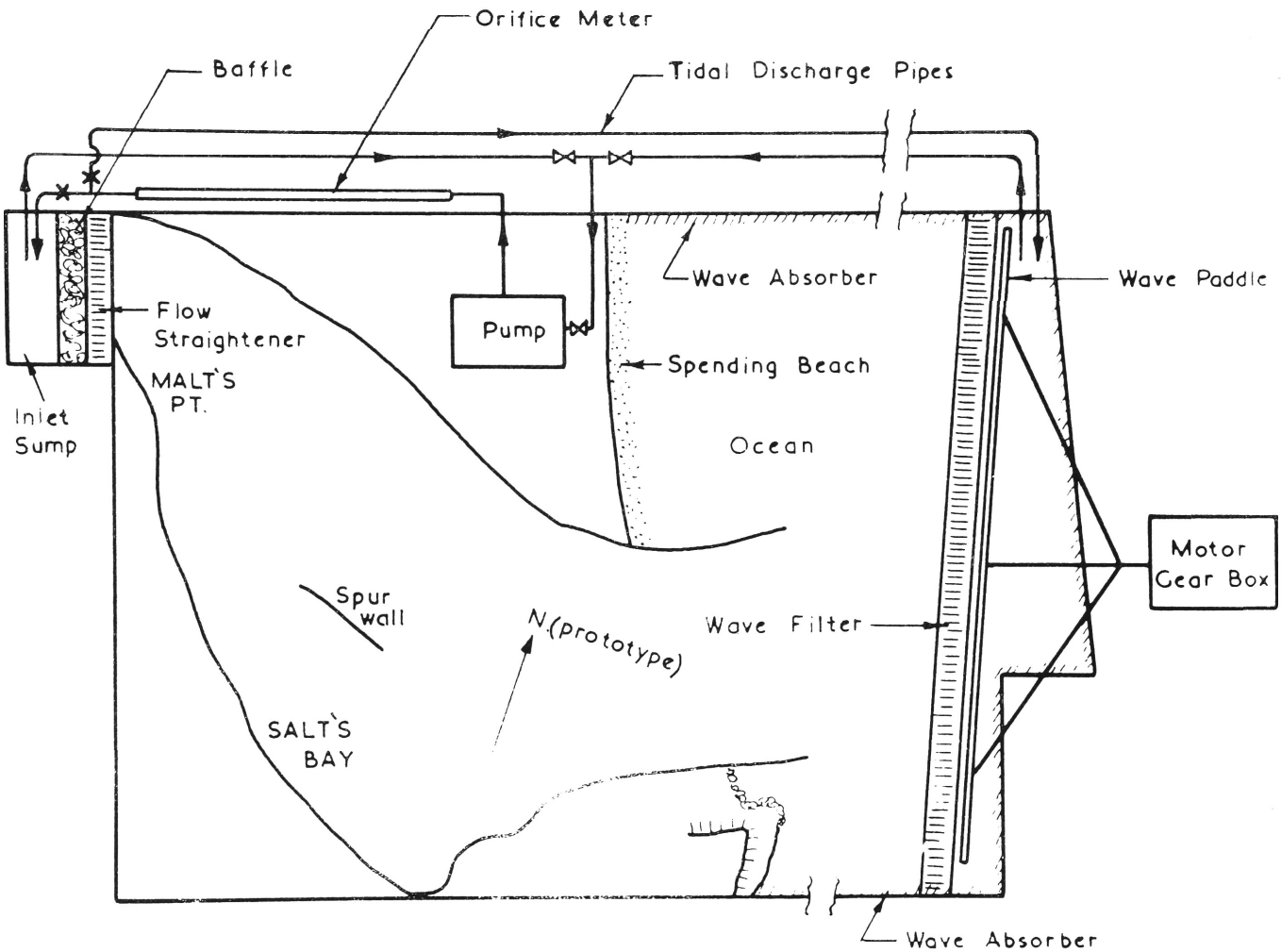

Figure 19: Diagram of Model Layout

wave scaling, where the wave height and length are both scaled to the vertical geometric scale, or depth scale (Gourlay, 1964). The wave height scale is taken as the vertical scale of the model and the wave length scale as the horizontal scale of the model:

$$\lambda_r = L_r \tag{5}$$

where λ = wave length

L = a horizontal dimension

and then, since the wave period is given by

$$\lambda = CT \tag{6}$$

where C = wave celerity

T = wave period

we find the scale of T as

$$T_r = \frac{\lambda_r}{C_r} = \frac{\lambda_r}{V_r} = \frac{L_r}{\sqrt{d_r}} \tag{7}$$

Since $L_r = 150$ and $d_r = 50$, $T_r = 21.2$, and the model period required to simulate a 10 second prototype wave is therefore about $\frac{1}{2}$ second.

The generally accepted formula relating wave length and velocity with water depth is

$$C = \sqrt{\frac{g\lambda}{2\pi} \tanh \frac{2\pi d}{\lambda}} \tag{8}$$

As d becomes large, this equation reduces to

$$C = \sqrt{\frac{g\lambda}{2\pi}} \tag{9}$$

which, in association with equation (6), $\lambda = CT$, yields the relation previously quoted for "deep water", $\lambda_o = \frac{g T_o^2}{2\pi}$ (Equation 2). It can be seen that for deep water Froude scaling with $C_r = \sqrt{d_r}$ will not give the same results in a distorted model as wave velocity scaling

with $C_r = \sqrt{\lambda_r} = \sqrt{L_r}$. However, where the wave length is great compared with the depth, as in very shallow water waves, equation (8) reduces to

$$C = \sqrt{gd} \qquad (10)$$

and it can be seen that Froude scaling gives the same results as wave velocity scaling, i.e. $C_r = \sqrt{d_r}$, which for the Lake Macquarie model is $\sqrt{50}$ or 7.07.

By reverting to the general wave formula (equation 8) we can estimate the discrepancies for the Lake Macquarie model. It is evident that, for the shallow depths encountered, conditions are fairly close to the shallow water case, but exact scales for various depths are shown in Table 3.

TABLE.3.

VELOCITY SCALES FOR WAVE ACTION BASED ON

$$C = \sqrt{\frac{g\lambda}{2\pi} \tanh \frac{2\pi d}{\lambda}}$$

Prototype 10 second waves		Model $\frac{1}{2}$ second waves		Wave Velocity scale
d-ft.	C-ft/sec.	d-ft.	C-ft/sec.	
18	23	0.36	2.45	9.4
12	19.5	0.24	2.24	8.7
9	17	0.18	2.05	8.3
6	14	0.12	1.77	8.0
4	12	0.08	1.50	8.0

From this table we see that the wave velocity scales are about 10 pc. higher than the Froudian velocity scale of 7.07 in the shallower depths encountered within the entrance, and the discrepancy increases in the deeper water outside the breakwaters. It is mainly within the entrance that we are interested in the similarity of wave and current scales, and a 10 pc. discrepancy should not create unduly large scale effects. The discrepancy is, of course, the result of the distortion of the model.

It is obvious that refraction, being dependent on wave velocity ratios from one depth to another, will not be reproduced exactly on the

model. A refraction diagram was constructed for the model waves from the 4 fathom contour, where the wave paddle is located, to the breakwaters.

Reference to Sections 3. 23 and 3. 24 and Figures 13 and 15 will show that, as a result of refraction, the rays for waves from east-north-east are bent to the north and those for waves from east are bent to the south, so that both sets of waves enter the breakwaters at a direction about 10^{o} north of east.

In the model, a wave paddle situated in about 4 fathoms (prototype) water depth is oriented perpendicular to 15^{o} north of east and produces waves with direction corresponding to the direction of most of the rays from east-north-east at the 4 fathom contour, and to the average of the directions of rays from east, which are more widely divergent as to direction. The model wave period is $\frac{1}{2}$ second. Figure 20 shows the refraction of $\frac{1}{2}$ second model waves from direction 15^{o} north of east at 4 fathoms from the 4 fathom contour to the breakwater entrance. The bending of the rays can be seen to be similar to that of east-north-east waves (Figure 13), the mean direction of waves at the entrance to the breakwaters being some 10^{o} north of east. Observation of Figure 15 shows that this direction is not vastly dissimilar from the direction of easterly waves at the breakwater.

As far as the breakwaters, therefore, model waves are reproducing prototype refraction quite well. Inside the breakwaters, refraction will be complicated by the existence of breakwaters. Within the entrance, where wave velocity scales are more truly representative of prototype conditions, differential refraction between model and prototype due to discrepancies of wave velocity scales will be even less than that outside the breakwaters.

As the waves in the model are entering the breakwaters at an angle, some reflection can be expected. This will not be important compared with other effects such as refraction. Since this is a distorted model, breakwaters built to geometric scale have their slopes increased by a factor of 3. All other things being equal, the steeper slopes on the model make better reflecting surfaces than the prototype slopes. However, since the degree of wave reflection is dependent on the wave steepness (or $\frac{\text{height}}{\text{length}}$ ratio) and since this is greater for the model than for the prototype, the model's reflecting power will be reduced on this account. The increase of reflection because of geometrical model

distortion and the decrease of reflection because of wave camber distortion are effects of the same order of magnitude which, operating in opposite directions as they do, can easily produce model reflection close to prototype reflection (Greslou and Mahe, 1954). The discrepancy between the Froudian scale and the wave velocity scales should not be enough to affect to any degree the reflection scale - up from model to prototype.

One of the effects of distortion of the model was to limit the wave height that could be used in the model in the following way. Wave breaking in deep water occurs when the stability of the wave crest can no longer be maintained, and this criterion can be expressed in terms of the maximum angle that can be supported at the crest. This angle is related to the steepness of the wave, or ratio of height h to length λ, and, though this relation varies somewhat with wave characteristics, the figure for maximum steepness of $\frac{h}{\lambda} = \frac{1}{7}$ can be taken as a fair guide. In prototype deep water, the wave length for a 10 second wave is about 500 feet, so that a wave height of 70 feet could be reached before breaking would occur. In the model, for a wave period of $\frac{1}{2}$ second, the wave length is about 1 foot and the maximum wave height for no breaking is therefore 1/7 foot. The highest model wave that could be maintained unbroken was found to be that corresponding to a prototype wave of 7 feet (which with a vertical scale of 1:50 agrees with the theory giving maximum wave of 1/7 ft. on the model). Thus although waves with wave height at 4 fathoms of up to about 9 feet from E. to E.N.E. have been shown capable of coming into Lake Macquarie Entrance without breaking on the bar, the highest wave that the model could reproduce was the 7 foot wave.

To estimate prototype conditions for higher waves, it is necessary to remember that both wave energy and littoral drift (rate of sand movement) are proportional to the square of the wave height (Savage 1949) while littoral current velocity is proportional to the first power of the wave height (Putnam et al, 1949). Thus a littoral current up to 30 pc. greater than that shown on the model with a 7 foot wave would prevail under 9 foot waves, while wave energy would be increased by 60 pc.

3.33 Model Construction

The model was constructed to suit the foregoing considerations. Figure 19 shows the basic features.

Tidal flow was provided by pumping to and fro between a sump

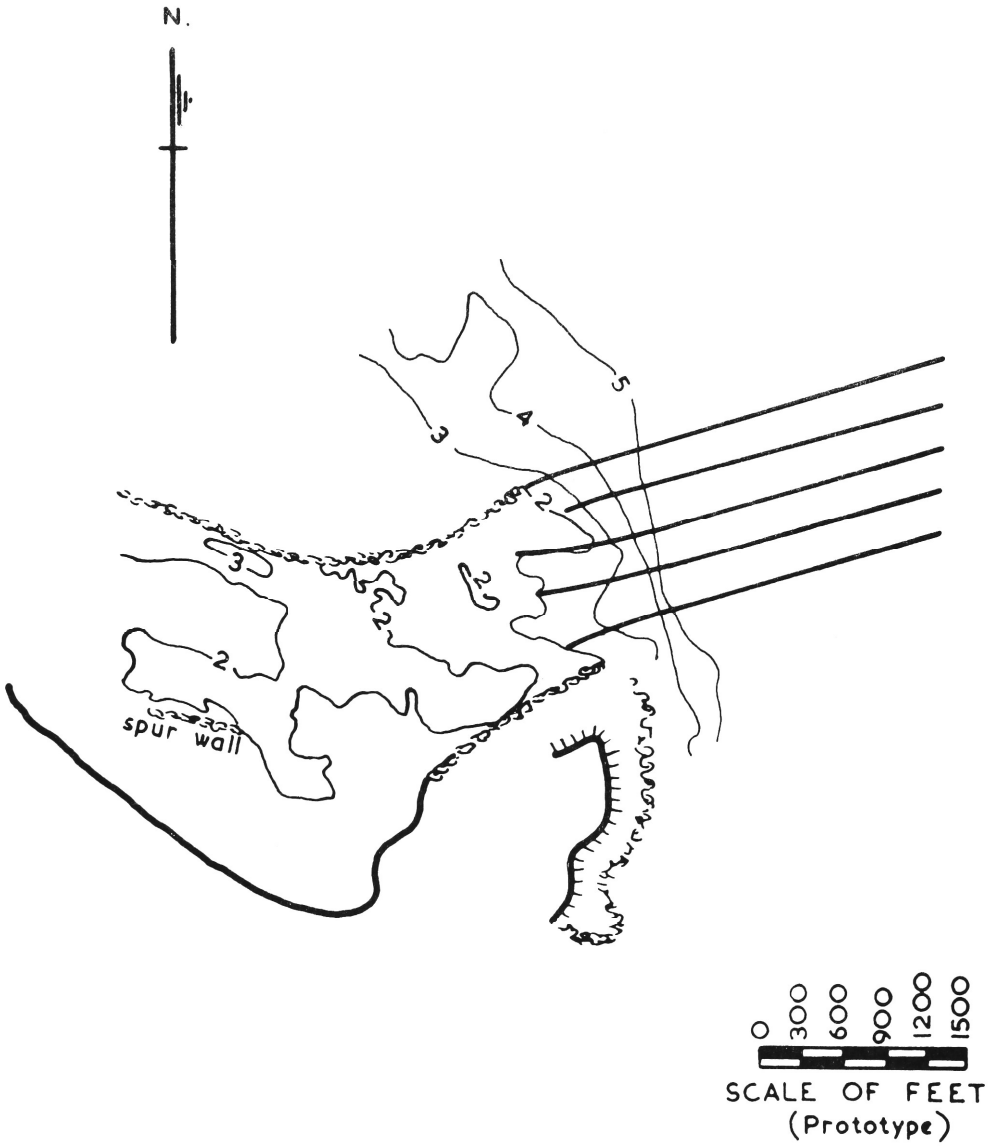

Contours in fathoms at mean high water (prototype)

Figure 20: Refraction Diagram for 1/2 second Waves from 15° N of E at 4 fathoms (Model)

upstream of Malt's Pt. and the body of water behind the wave paddle. An orifice meter in the circulating rig metered the flow.

Waves were generated by a simple hinged paddle located at about the 4 fathom contour and oriented to give waves with direction 15° north of east at that location. With the wave paddle located in a depth where the waves have already been affected by the bottom and the water orbits have been changed from the circular paths characteristic of deep water waves to the elliptical paths characteristic of shallow water waves, the wave paddle should theoretically have movement both top and bottom. However, experience has shown that in such a small water depth a wave generated by a paddle whose bottom is not free to move in translation will attain the characteristics of a shallow water wave in a matter of some feet, and therefore, for ease of construction, a paddle rotating about hinges fixed in the model bed was adopted. The paddle was driven by a mechanism which produced a motion very close to simple harmonic at the top of the paddle, the motive power being supplied by a 2 H. P. motor through a variable drive and suitable reduction gears. With the variable drive the period of the waves could be altered if necessary, and by varying the throw of the crank to the paddle the height of the waves could be changed.

To complete the details of model construction, it may be noted that the surface was moulded between vertical galvanised iron templates set at about 2 foot intervals in the model. These were laid on a series of rails suitably located and carefully levelled; sand was used for filling to within an inch of the top and a cement mortar cap was then screeded to be level with the templates. Breakwaters and training walls of no fines concrete were added. Wave absorbers, consisting of rubberised hair, were attached to any steeply sloping areas, such as the walls of the wave basin, to reduce spurious reflections. A wave filter of folded birdwire was placed in front of the paddle as is customary, but it proved unnecessary, as quite pure waves were found when it was removed. Because of the swirl in the sump at the upstream end of the model a baffle and flow straightener were provided to produce good entry conditions into the model. No similar precautions were needed at the seaward limit, for the tidal flow entered between the breakwaters after passing under the wave paddle with quite an even distribution.

4. Model Tests

4.1 Scope of Model Tests

The model was operated in its natural condition with waves and

tidal currents simulated, and measurements of waves and currents along the southern shoreline taken. These measurements were then repeated with various structures in the model and some qualitative tests were also made of sand movement along the shore. The structures tested were:-

(1) Short spur dyke running westerly from the inner end of the southern breakwater.
(2) Restoration of old spur running easterly from the western end of the beach.
(3) Series of northerly spur dykes (groynes) located along the beach.
(4) Wave reflecting pile groups offshore from the beach.
(5) A submerged breakwater in Salt's Bay running east-west.

Currents were measured either by timing the passage of a dye-front or by a small laboratory current meter. Waves were measured directly against a graduated scale.

4. 2 Wave Heights

4. 21 Natural Conditions

Since model tests were performed before field data relating the times of high and low tide and maximum strengths of ebb and flow had been obtained, tests were performed at mean high water, since higher waves can penetrate the entrance at times of high water. It is obvious from the field data that certain conditions applied to the model cannot prevail in nature. For instance, by reference to Figures 2 and 3 of Appendix I, it can be seen that maximum tidal outflow occurs about the time of low water and maximum tidal inflow about the time of high water. Therefore, the combination of maximum tidal outflow and high water represented in Figure 22 does not normally occur in nature. However, it is a worse case than outflow combined with low water as far as waves are concerned, and, as can be seen from Figures 27 and 28, current patterns are similar: therefore, since the outflow tests made at high water do not show as critical a case as inflow tests at high water, by so much more would the natural conditions be less critical with outflow than with inflow.

The results for the condition of outflow combined with high water shown in Figure 22 are presented here as an interesting indication of the effect of an opposing current in steepening waves and making them break prematurely. It can be seen by comparison between Figures 21 and 22 that the wave heights throughout the entrance are substantially lower when there is an opposing current. It will be remembered that,

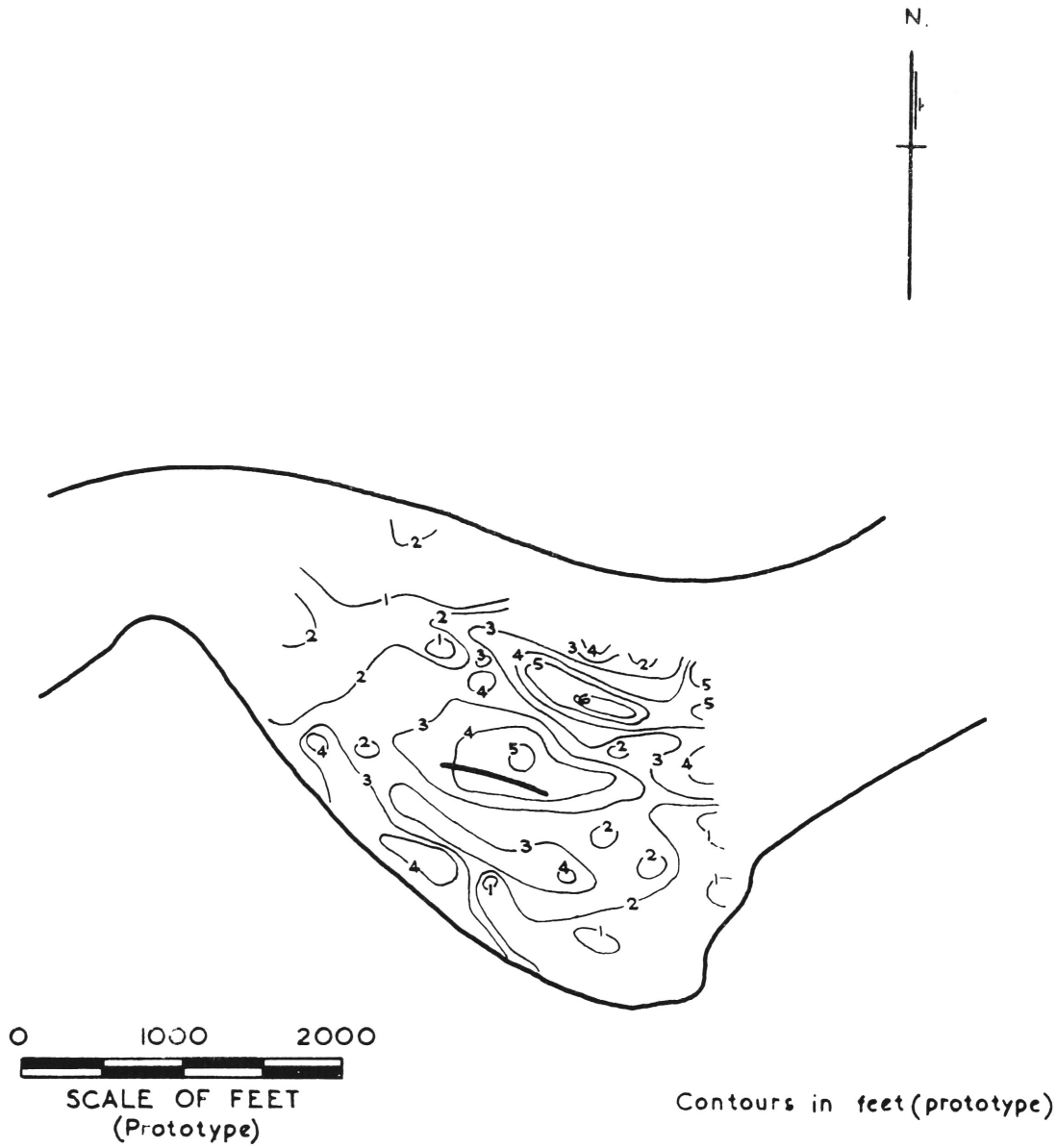

Figure 21: Wave Height Contours in Lake Macquarie Entrance for 7 foot Ocean Wave. No Tidal Discharge. Water Level at M.H.W.

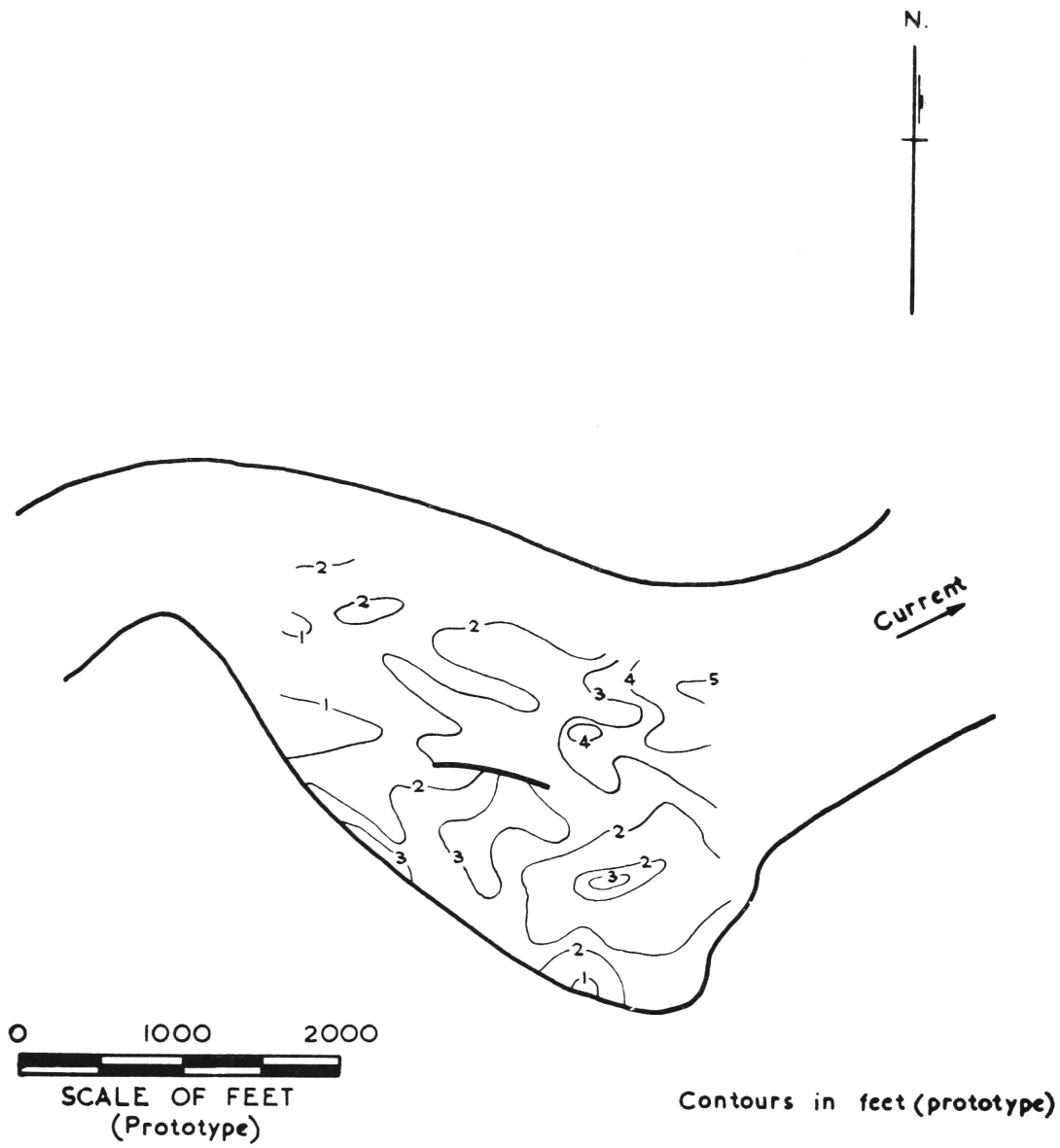

Figure 22: Wave Height Contours in Lake Macquarie Entrance for 7 foot Ocean Wave and Tidal Discharge 26,500 c.f.s. Outflow. Water Level at M.H.W.

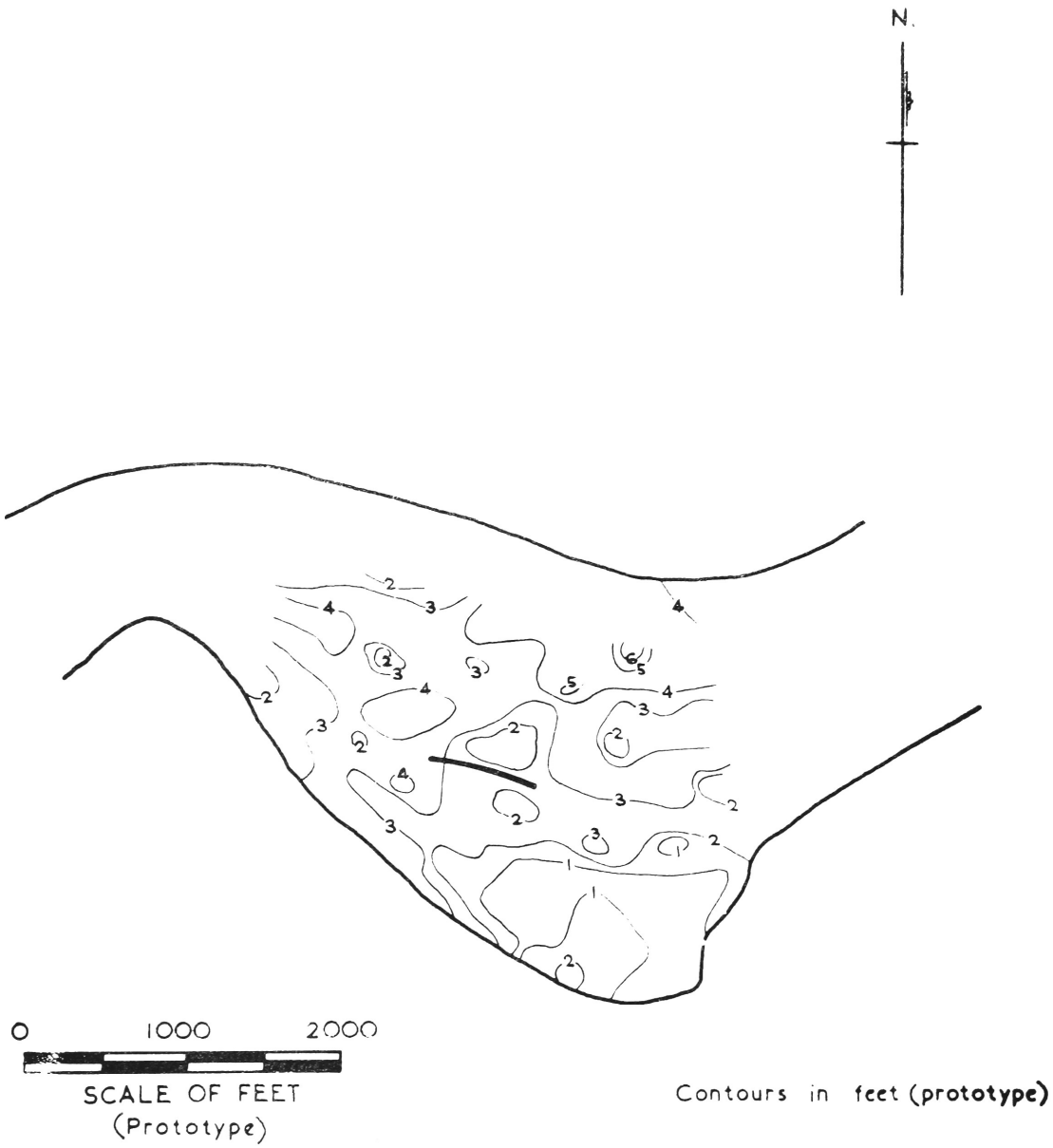

Figure 23: Wave Height Contours in Lake Macquarie Entrance for 7 foot Ocean Wave and Tidal Discharge 26,500 c.f.s Inflow. Water Level at M.H.W.

in the model, the waves representing 7 foot ocean waves are close to their limiting steepness, and any steepening will therefore result in breaking and dissipation of energy, so that less wave energy will penetrate the entrance. In the prototype, of course, a 7 foot 10 second wave is not close to its limiting steepness and the tidal outflow will not have such a marked effect as far as causing waves to break in deep water is concerned. The fact that the opposing current has increased the wave height will increase the chances of breaking on the bar, and, since outflow currents are associated with lower water levels, it is probable that waves substantially smaller than 7 feet (ocean) height will break on the bar during the ebb.

The lengthening and smoothing of waves caused by an inflowing tide which operates in the sense of propagation of the waves has no such marked effect, since it does not induce a critical condition. This can be seen by comparison of Figures 21 and 23. It will be noted that because of the reduction in wave height due to the assisting current, ocean waves of somewhat greater height will be able to penetrate the entrance than if there were no current. Figures 21 and 23 show that an assisting current causes a certain redistribution of wave energy within the entrance, higher waves penetrating farther towards Malt's Point, while directly south of the spur wall the wave height is slightly decreased. The two conditions are, however, quite similar, and, since the inflow current creates a worse condition as far as drift along the shore is concerned, the combination of inflow with high water was chosen as the critical condition and testing of structures to mitigate erosion of the shore was subsequently carried out for this case.

Figure 23 shows that, under natural conditions for waves from directions E. to E. N. E. , for a 7 foot ocean wave with tidal discharge 26,500 c. f. s. inflow, there are induced along the shore of Salt's Bay waves ranging in height from between 1 and 2 feet in the protected eastern corner to between 3 and 4 feet directly south of the spur wall, and decreasing again to between 1 and 2 feet near Malt's Point. The currents prevailing along the shore under natural conditions will be discussed later, but first we can consider the effect on wave height of various structures examined in the model. It will be noted that no wave measurements were made for one of the proposed structures, this being the series of northerly groynes set along the southern shoreline. This is because the waves will be affected only in the area local to the groynes, and the purpose of the groynes is not to alter wave heights, but rather to retain drifting sand.

4. 22 Spur wall extended westerly to shore, all at level of present spur wall

This is along the alignment of the wall that existed from 1880 to some time between 1921 and 1929 when the first break in the wall occurred. During that time the wall was above high water, whereas its present level is at least 2 or 3 feet below M. H. W., and this test was made with the restored wall also at this lower level.

With the model operated at M. H. W. this low wall offers little resistance to the waves and, as can be seen from Figure 24a, the wave heights measured on the model showed no difference from those measured under natural conditions.

4. 23 Spur wall extended as above and raised throughout its length to above M. H. W.

Figure 24b shows that this higher wall decreased the wave heights south of the spur wall to between 1 and 2 feet (from 3-4 feet under natural conditions) while raising wave heights slightly in the eastern corner of the bay, from 1-2 feet under natural conditions to 2-3 feet.

4. 24 Existing spur wall raised above M. H. W.

In case simply raising the level of the existing spur might produce similar results as far as wave heights are concerned, this situation was tested, but it was found that wave heights were not nearly so markedly reduced, some 3-4 foot waves still remaining in the area south of the spur (Figure 24c).

4. 25 Spur wall extended easterly, all above M. H. W.

To see whether an easterly extension of the spur wall decreased wave entry into Salt's Bay, a 200 foot easterly extension was built, the wall being raised along its length to above M. H. W. Wave heights directly south of the spur were reduced to between 1 and 2 feet and this reduction in wave height extended farther east than before (Figure 24d) but there were still some 3-4 foot waves west of this. It seems that some westerly extension of the spur is required to reduce the waves in this western area.

4. 26 Pile groups between the spur and the southern shore

Wave reflecting pile groups, each group about 100 feet long, were tried as a method for reducing waves. Various configurations were tried until a layout which would reduce wave heights to about 2 feet

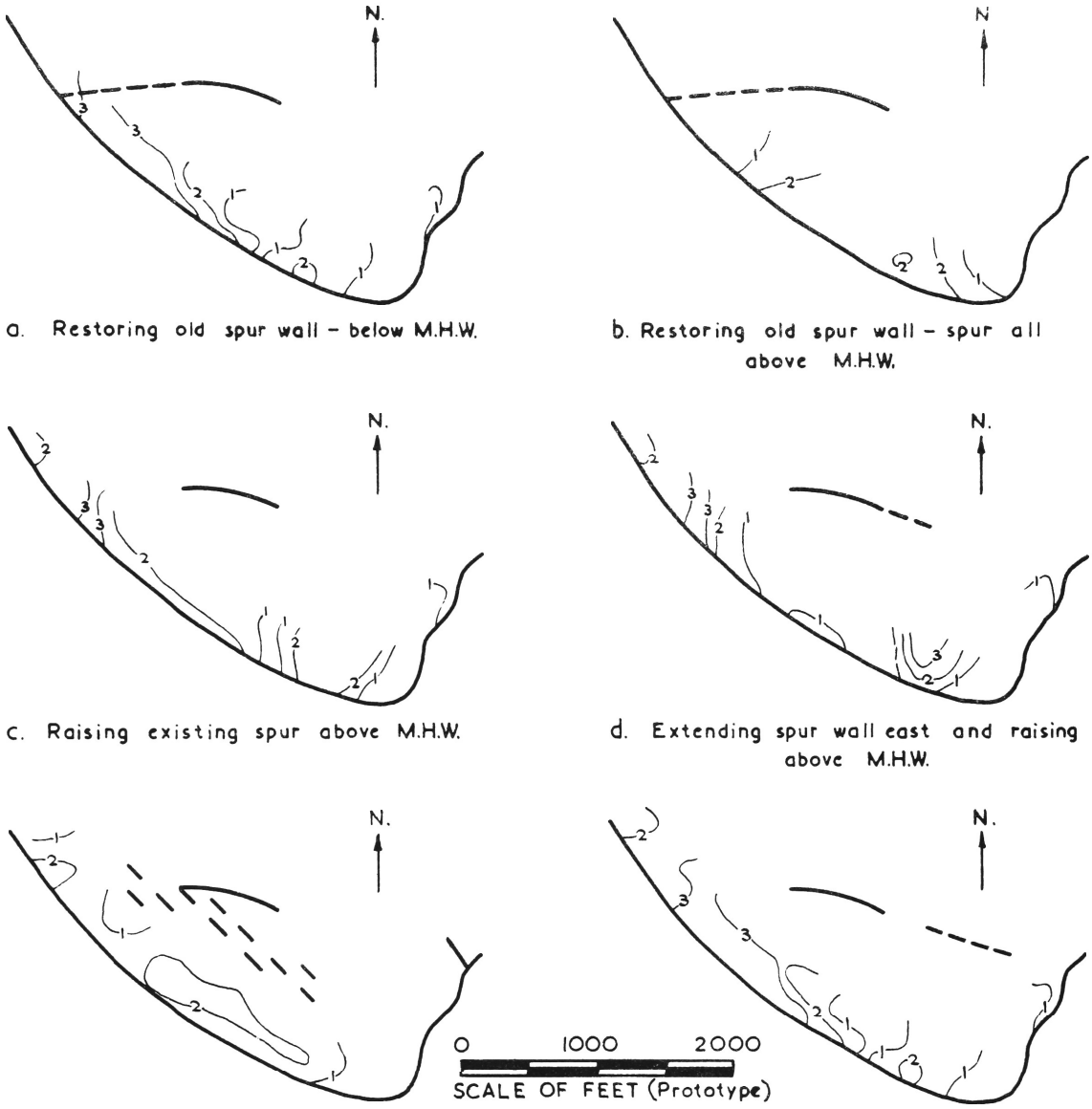

Figure 24: Wave Height Contours in Salt's Bay with some Structures Tested for Mitigating against Erosion.

Ocean Wave Height	7 ft.
Tidal Discharge - Inflow	26,500 c.f.s.
Water Level	M.H.W.

using as few piles as possible was found. This layout is shown in Figure 24e. It will be noted that the test conditions recorded included a dyke or small spur at the landward end of the southern breakwater. Since the effect of dykes placed in this area was purely local, the results shown for wave heights along the southern shore can be taken to apply for the pile group structure with or without the dyke.

4. 27 Submerged breakwater east of spur wall

Submerged breakwaters raised to mean water level with lengths up to the total length between the spur and the southern breakwater and widths as great as 100 feet (prototype) were tried with no success, so further testing of this idea was abandoned. Figure 24f indicates the breakwater location and shows no reduction in wave heights below natural conditions.

4. 28 Dyke at landward end of southern breakwater

Short dykes 100 to 200 feet in length were tried at various orientations, extending from the landward end of the southern breakwater. One of these is shown in Figure 24e. Another is shown in Figure 24g with a raised and extended spur wall as discussed in 3. 3. Comparison of Figure 24g with 24b shows how little effect such a spur dyke has on wave heights along the southern shoreline.

4. 29 Summary

From the above it is seen that two proposals are effective in reducing wave heights. These are (1) westerly extension and raising of the spur wall togehter with some short easterly extension, and (2) wave reflecting pile groups between the spur and the shore. Since it is not considered that reduction of wave action is the only method, or even the best method, for ensuring stability or accretion of the shore, further discussion of the relative merits of the various methods will be delayed until currents and sand drifts have been considered.

4. 3 Currents

4. 31 Natural Conditions

Currents are induced in Salt's Bay mainly as a result of waves and tides. These have been examined both separately and together.

The currents associated with waves are the mass transport current, which results from the fact that the water particles move in open rather than closed orbits, and the littoral current which results when

waves strike the shore obliquely. Of these, the one which interests us most is the littoral current which is generated along the southern shore by waves coming into Lake Macquarie Entrance. From model measurements the strnegth of this current was found to be between 1 and 2 feet per second, as can be seen from Figure 25. This littoral current flowed west from a point south of the eastern end of the spur wall. East of this point, there was comparatively little current, a very slow water movement which transported water in weak eddies prevailing.

When an ebb tide was superimposed on the waves, the current pattern shown in Figure 26 was found. Water flowing along the southern shore of Salt's Bay formed part of a reverse eddy which, with or without waves, was always associated with outflowing tides. This reverse eddy covered a substantial area, including all of Salt's Bay. Figures 27 and 28 show the current patterns found at both Mean High Water and Indian Springs Low Water for an ebb tide with no waves. These show only slight variations from Figure 26. Some measurements of currents at Mean High Water with ebb tide and no waves are given in Figure 4 of Appendix I. From this figure, by multiplying current speeds found on the model by the velocity scale of $\sqrt{50}$ or 7.07, it can be seen that a westward current up to about $\frac{1}{2}$ ft. per second exists along most of the southern shoreline. Figure 26 shows that with waves and ebb tide acting together, the westward currents along the southern shore are similar in strength to those found for waves only, that is, up to 1 or 2 feet per second in the westward section with a very slow water movement farther east.

With a flood tide, a reverse eddy was also formed (Figure 29), but this covered only a limited area compared with that covered by the large reverse eddy associated with the ebb tide, and was restricted to the south-eastern corner of Salt's Bay, near the landward end of the southern breakwater. Thus we find a west flowing current along most of the southern shore during all stages of the tide. With the flood tide, the speed of this current is substantially greater than under other conditions, being up to 3 feet per second. From Figure 30 (and also Figure 5 of Appendix I) it can be seen that this current pattern persists even when there are no waves, and from Figure 5 of Appendix I the speed of the westward current can be computed - figures of between $\frac{1}{2}$ and 1 foot per second are found. Figure 31 shows the current pattern that would exist at I. S. L. W. with a flood tide and no waves, though the combination of flood tide and low water is of course unnatural, and this figure is included only for interest.

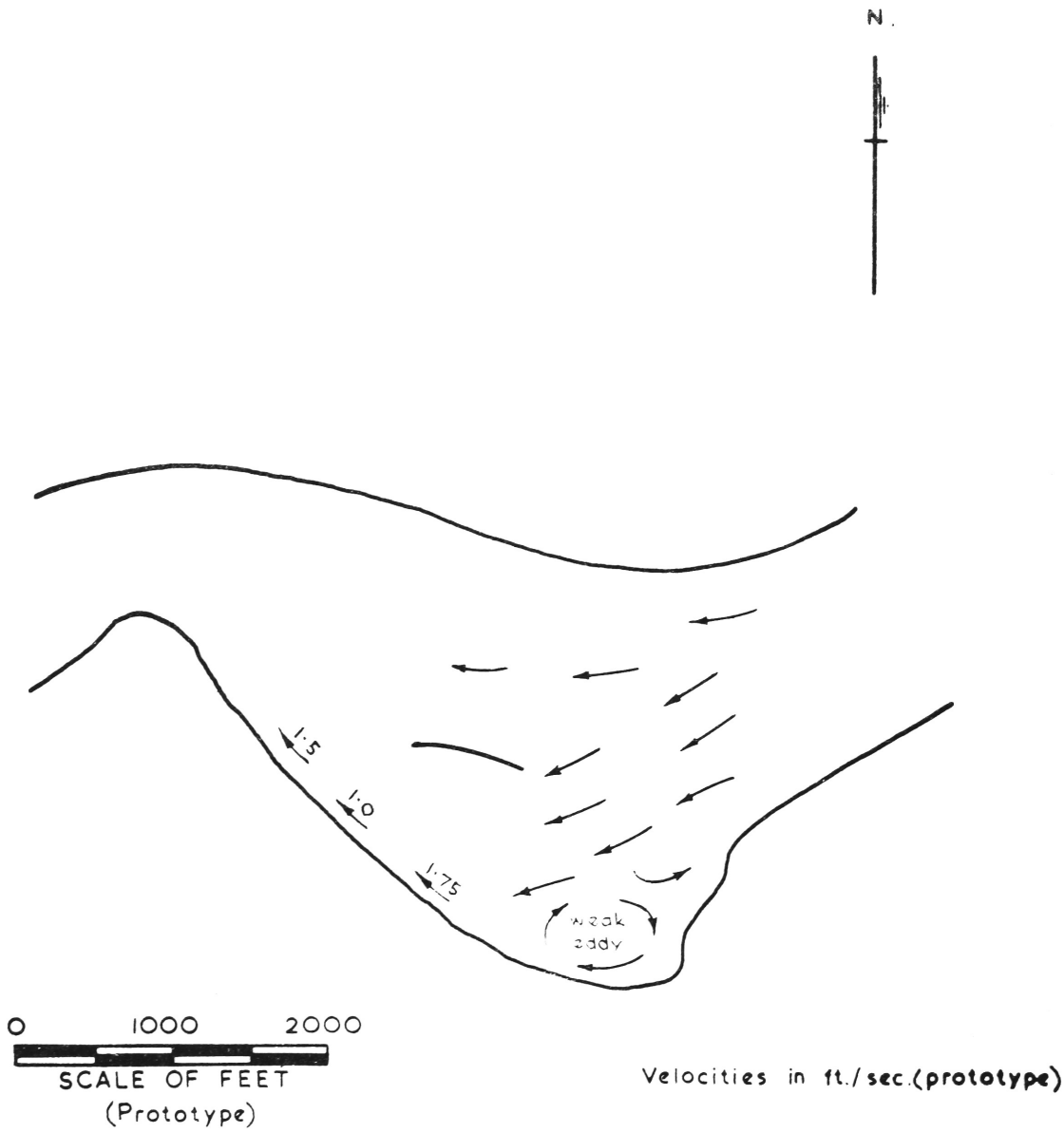

Figure 25: Wave Induced Currents in Lake Macquarie Entrance for 7 foot Ocean Wave. No Tidal Discharge. Water Level at M.H.W.

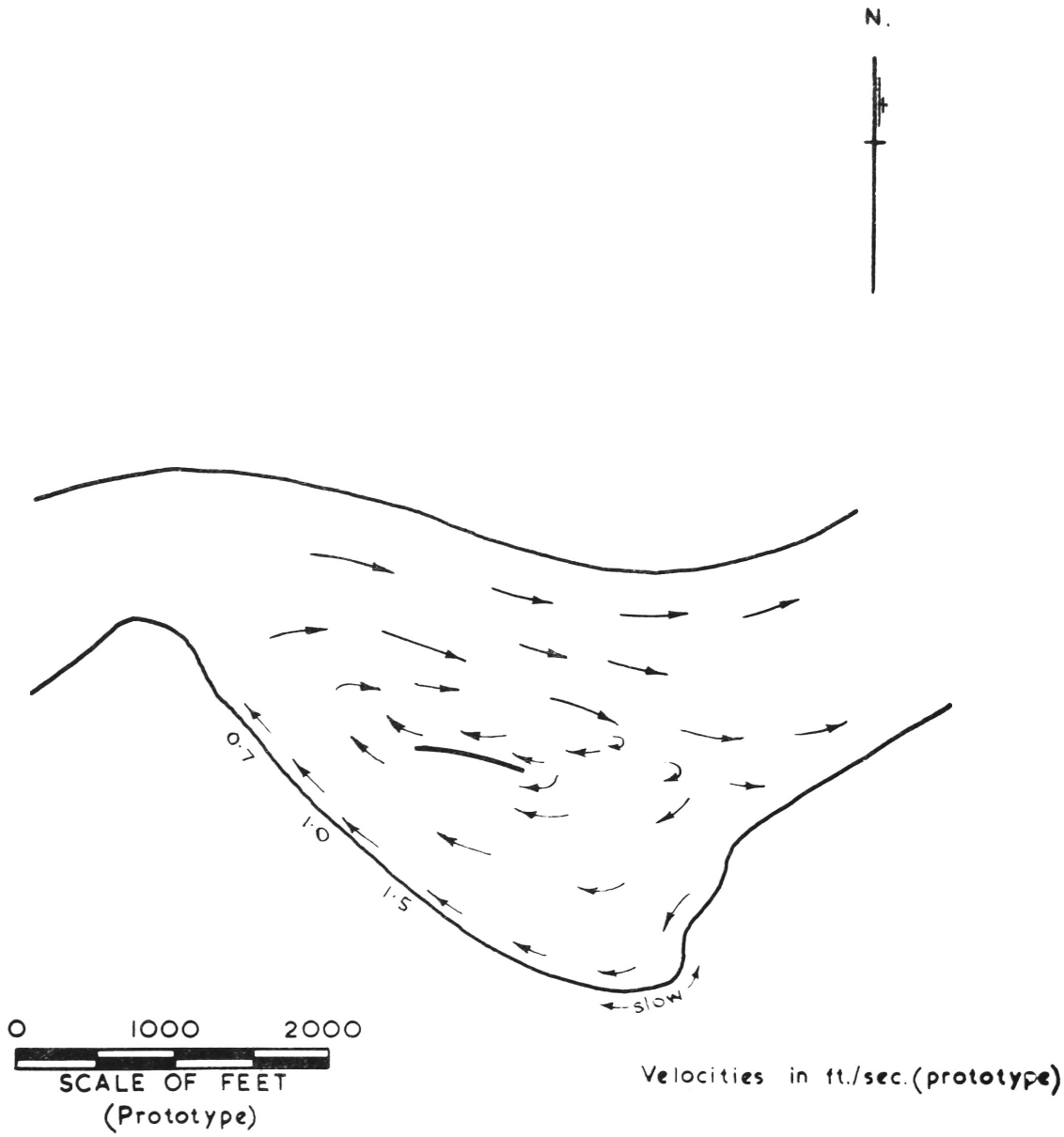

Figure 26: Currents in Lake Macquarie Entrance for 7 foot Ocean Wave and Tidal Discharge 26,500 cfs Outflow. Water Level at M.H.W.

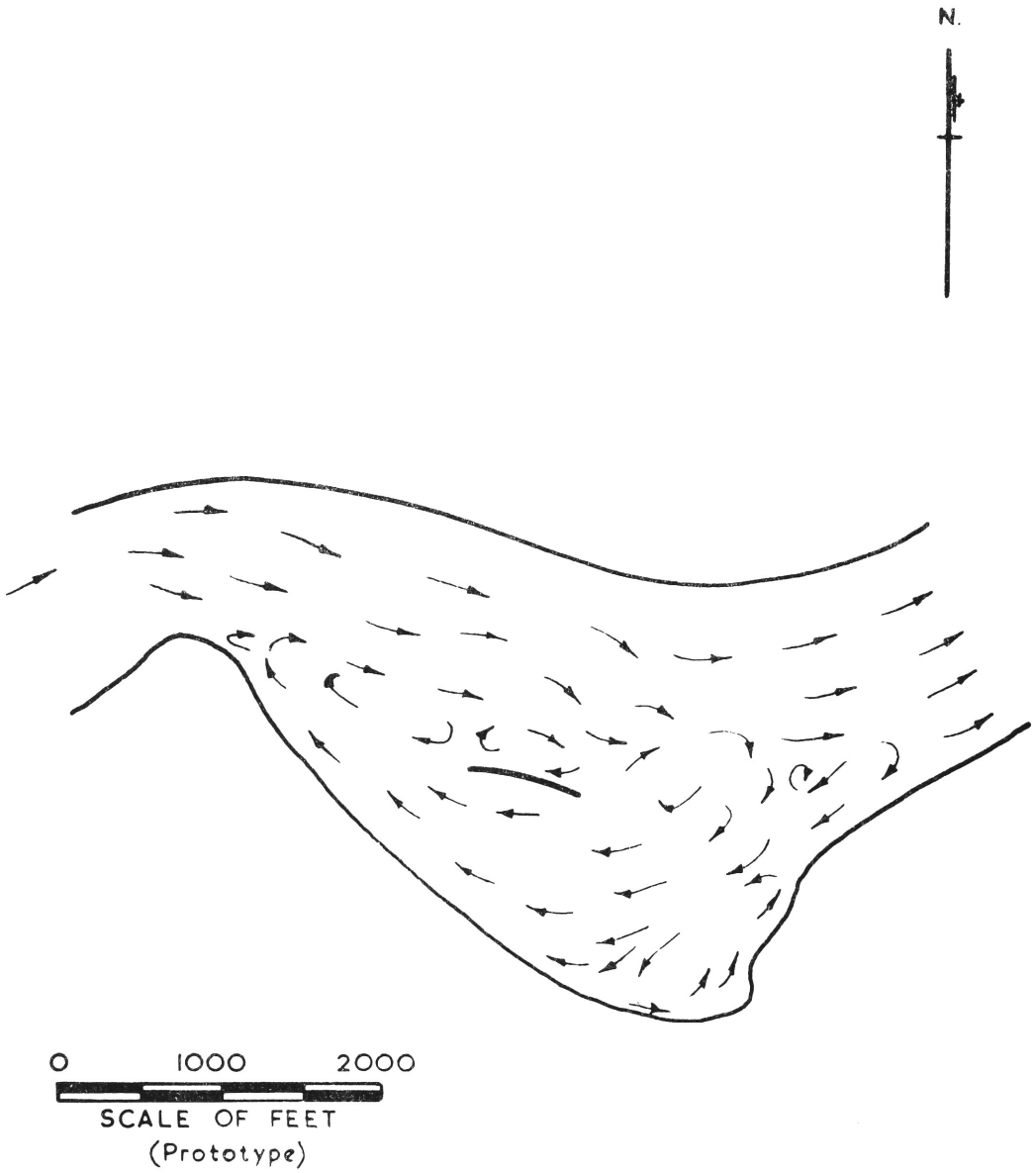

Figure 27: Current Pattern in Lake Macquarie Entrance for Tidal Discharge 26,500 cfs Outflow. No Waves. Water Level at M.H.W.

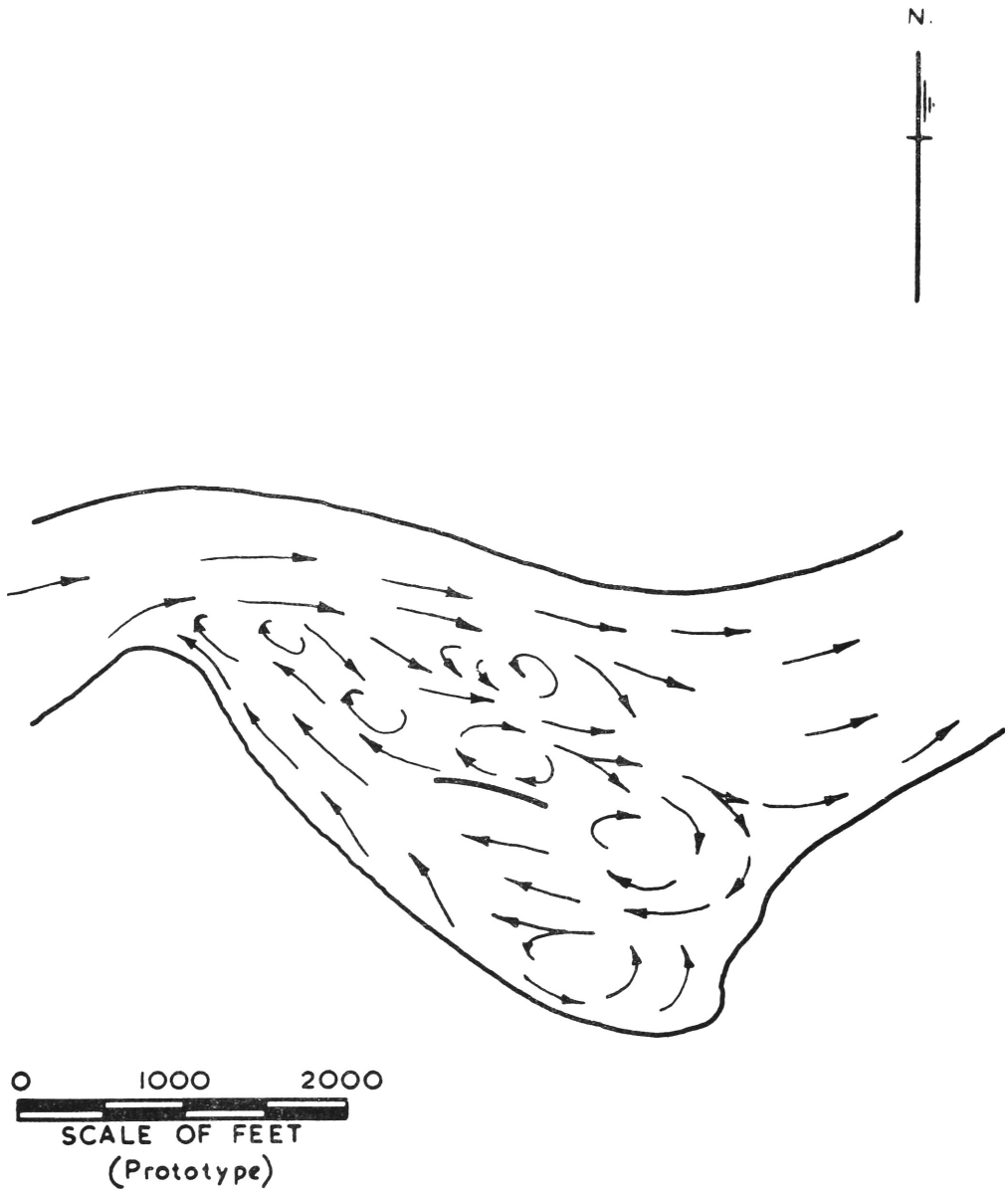

Figure 28: Current Pattern in Lake Macquarie Entrance for Tidal Discharge 26,500 cfs Outflow. No Waves. Water Level at I.S.L.W.

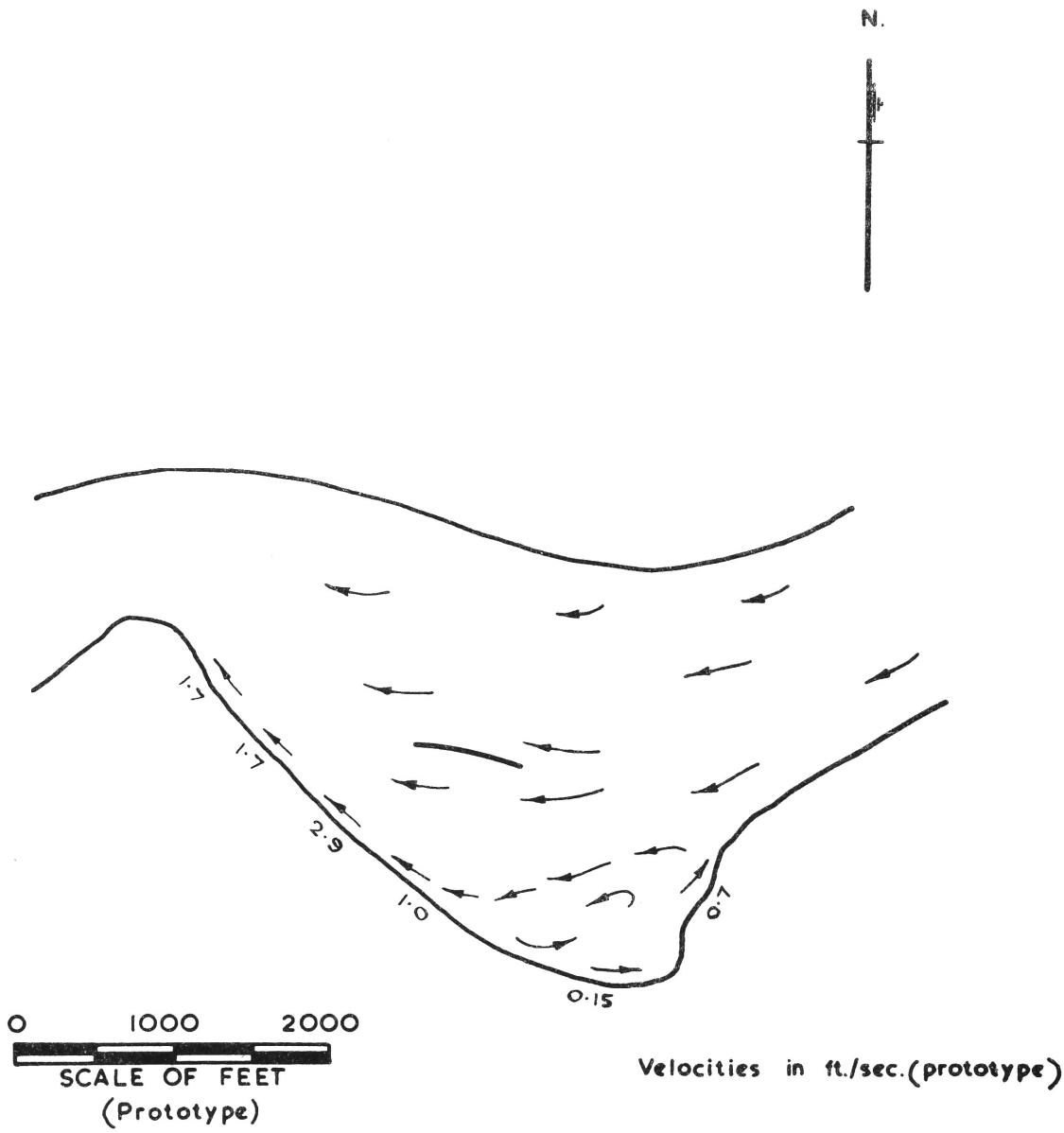

Figure 29: Currents in Lake Macquarie Entrance for 7 foot Ocean Wave and Tidal Discharge 26,500 cfs Inflow. Water Level at M.H.W.

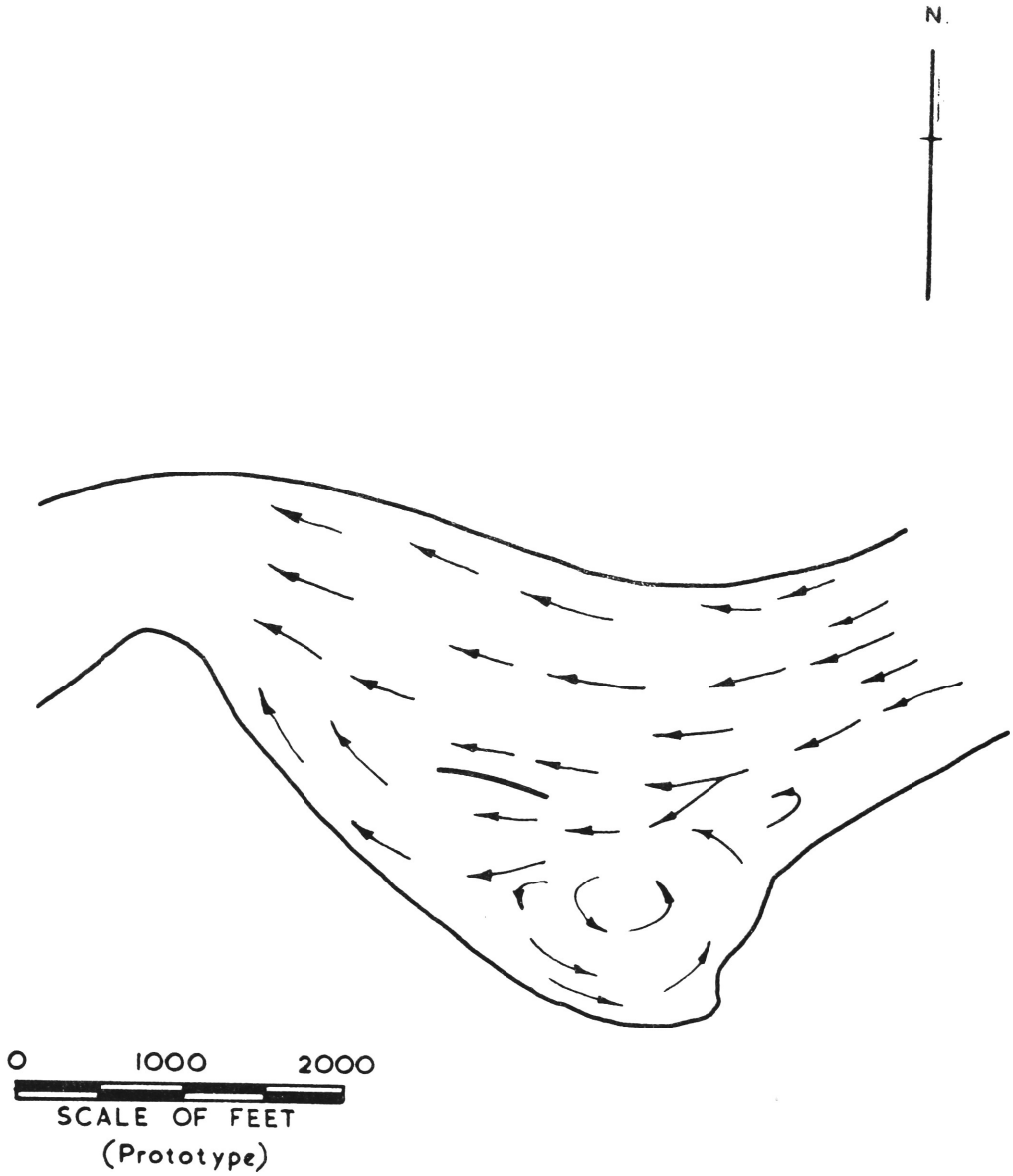

Figure 30: Current Pattern in Lake Macquarie Entrance for Tidal Discharge 26,500 cfs Inflow. No Waves. Water Level at M.H.W.

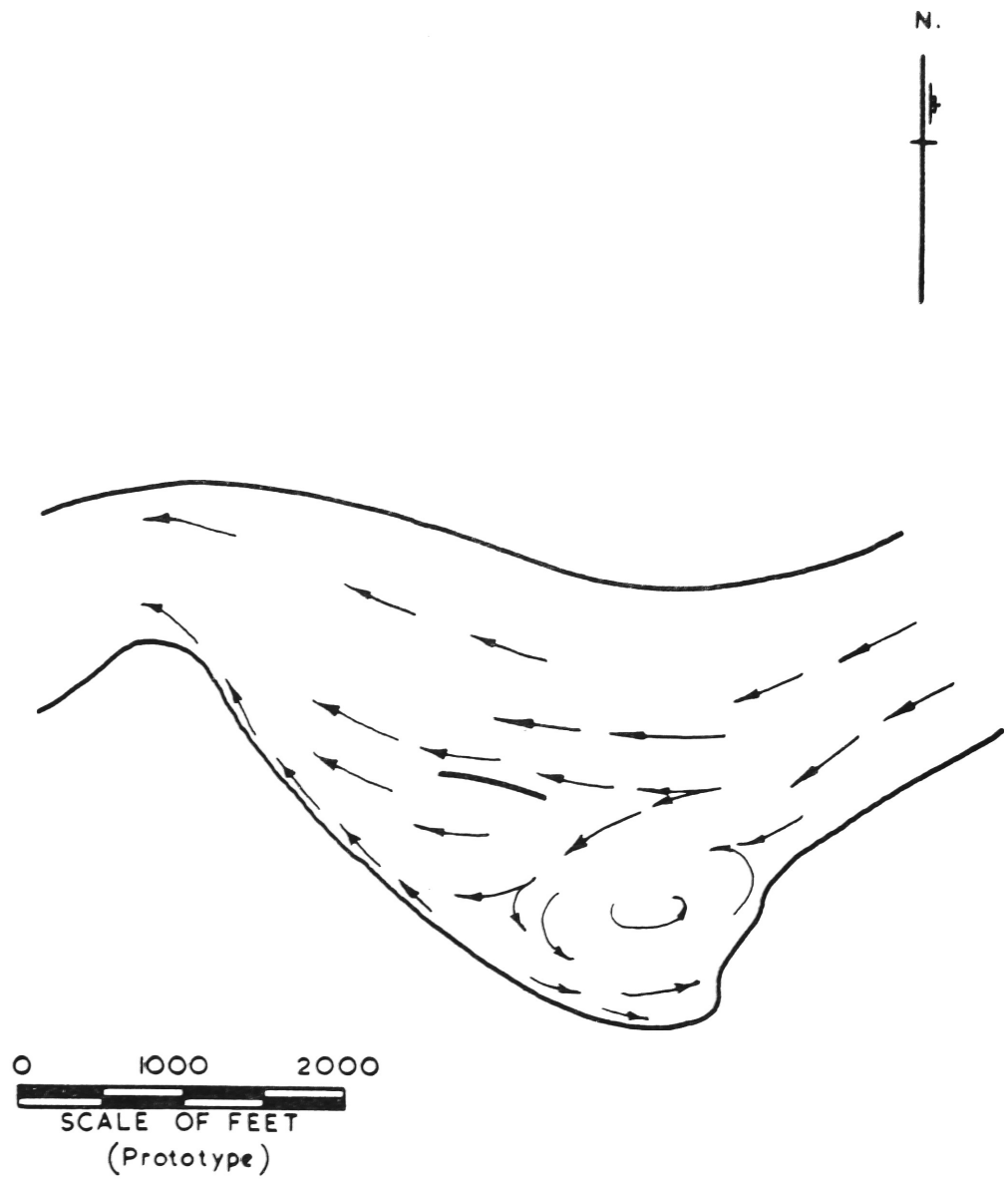

Figure 31: Current Pattern in Lake Macquarie Entrance for Tidal Discharge 26,500 cfs Inflow. No Waves. Water Level at I.S.L.W.

Table 4 summarises the foregoing.

TABLE 4.

WESTWARD CURRENTS ALONG SOUTHERN SHORE OF SALT'S BAY.

Waves and Tides	Current Speed (ft/ sec.)
Waves only (7ft.)	1 to 2
Ebb tide only (26,500 cfs)	$\frac{1}{2}$
Flood tide only (26,500 cfs)	$\frac{1}{2}$ to 1
Ebb (26,500 cfs) + waves (7ft)	1 to 2
Flood (26,500 cfs) + waves (7ft)	2 to 3

These currents are strong enough to transport considerable quantities of sand, particularly since the turbulence present even with low wave action will help in raising the sand into suspension and thereby make it available to the current.

The persistence of the west flowing current along the shore made the idea of a groyne field attractive. The necessity for careful design of any such groyne field cannot be over-emphasised. Many instances are found where groyne fields have not only failed to achieve their purpose but have caused major damage. Nor is it considered reasonable to extrapolate from a distorted fixed-bed model such as the one that has been used for this investigation to obtain the final design of a groyne field. The best method of attacking the problem might be to evolve a design based on a perusal of recent literature with attention to known successes and failures in the field. The design could possibly be checked on the model either in its fixed bed condition or with some of the bed removed and loose material substituted - the usefulness of such model testing would have to be investigated.

In the meantime, some very rough tests of sand movement have been made on the existing model for natural conditions and the condition with restored and raised spur wall as well as for a groyne system. These will be discussed in Section 4. 4

4. 32 Spur wall restored and raised to above M. H. W.

Under these conditions, Salt's Bay becomes a closed off bay and it is impossible for a continuous current to flow through between the old spur and the southern shore as it does under natural conditions.

The flow of water entering Salt's Bay becomes an eddy as shown in Figure 32a, with a velocity considerably less than the velocities previously measured. With this lower current speed combined with reduced wave heights (Ref. Section 4. 23), a wave-trap action can be expected, and sand carried by the current will deposit in the calm area at the western end of the bay.

4. 33 Wave reflecting pile groups

Currents were also observed with pile groups located as described in Section 4. 26. The currents are shown in Figure 32b To the east, currents are markedly reduced, but a west flowing current with speed up to nearly half of that found for natural conditions still exists in the western end of the bay.

4. 4 Sand Movements

4. 41 Natural Conditions

It should be noted that nothing but a rough idea of the movement of sand on the prototype can be gleaned from these tests, firstly because, with a fixed bed model, any sand added must alter the configuration of the shoreline making it extend farther into the water than in nature, and secondly because no attempt has been made to scale the movable material. In fact, ordinary beach sand was used.

Sand was evenly spread along the southern shoreline being tapered from the high water mark to a distance about 1 foot out from the shore. The model was left running for several hours with waves corresponding to 7 foot ocean waves in the prototype and a tidal inflow corresponding to 26, 500 c. f. s. prototype. At the end of the test, the sand width had reduced considerably immediately south of the eastern end of the spur wall, and increased towards Malt's Point. Some sand had continued past Malt's Point and collected in the inlet sump. In the south eastern corner of Salt's Bay, the edge of the sand had steepened appreciably and receded somewhat, but the cross-sectional area of the sand seemed to remain fairly constant, indicating no net loss or gain in this area. These results could be expected from a study of the currents.

4. 42 Restored and raised spur wall

For this condition, the test showed similar sand movements in the south-eastern corner and also, as before, a removal of sand from the area south of the eastern end of the spur wall. However, the sand that under natural conditions, had moved to the Malt's Point area was caught

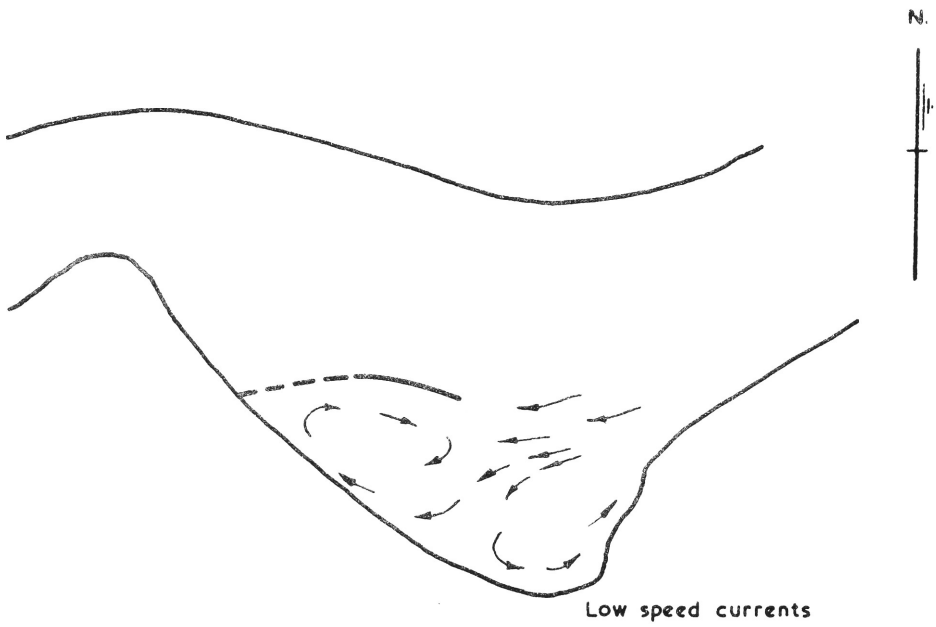

a. Restoring old spur wall and raising spur above M.H.W over entire length

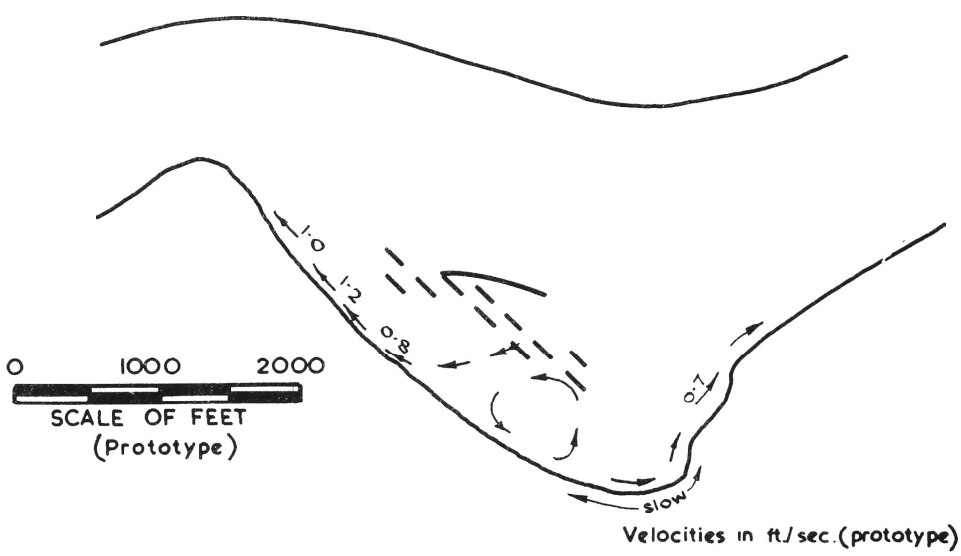

b. Wave reflecting pile groups

Figure 32: Current Patterns in Salt's Bay for 7 foot Ocean Wave and Tidal Discharge 26,500 cfs Inflow. Water Level at M.H.W. Structures Installed

by the restored spur wall, and a substantial sand build-up occurred in the corner between the shore and the spur. There is no reason to presume that a similar build-up will not also occur in the prototype. The time scale for such a build-up cannot be predicted from the model. Were the natural building rate not as rapid as desired, dumping of sand anywhere west of a point south of the eastern end of the spur wall could be undertaken to encourage it.

4.43 Groyne field

The groynes used on the model corresponded to 100 feet prototype length and were spaced 300 feet apart (prototype). They were sloped from mean high water at the same slope as the offshore bed, and were oriented at an angle between normal to the shore and normal to the wave fronts. (It will of course be appreciated that the above should not be taken as a basis for design of a groyne field). After the test, a build-up of sand was found on the updrift side of each groyne with some erosion on the downdrift side. The latter can be controlled by proper design. There was a marked reduction in the amount of sand reaching the Malt's Point area and travelling beyond Malt's Point into the sump.

5. Conclusions

As a result of this study the following conclusions have been reached.

5.1 History

Historically, the southern shore can be divided into two regions as far as erosion is concerned. In the south-eastern corner of Salt's Bay, extending for about 1000 feet from the landward end of the southern breakwater, lies a region where erosion is known to have been active during the last decade. To the west of this, extending to Malt's Point, lies a sandy beach backed by low-lying ground. Shoreline surveys for the years 1879, 1914, 1921, 1929 and 1954 indicate that, subsequent to the building of breakwaters and training walls in 1879, some changes in topography occurred as the shore adjusted to an equilibrium with the altered conditions. Changes seem to have been gradual up to 1921, but between 1921 and 1929 a break occurred in the wall, and the shoreline receded considerably at some time during the period 1929 to 1954. There are no surveys since 1954, so that it is not known whether the shore has reached its equilibrium position under the present conditions.

5.2 Wave Action

Waves from north-east to east have the most pronounced effect. Waves from north-east are limited in height and period because a headland to the north prevents ocean swell from reaching the entrance. Waves generated between this headland and the entrance are limited, because of the short fetch, to periods of about 6 seconds and heights of up to 5 or 6 feet (significant wave height) at the breakwaters. Ocean waves approach the entrance from east-north-east to east with periods generally in the range 6 seconds to 14 seconds and heights up to 30 feet. The higher waves will break seaward of the bar and so dissipate much of their energy. The maximum height of wave that can cross the bar without breaking is about 8 feet. Model waves were scale replicas of a prototype wave with height 7 feet and period 10 seconds with direction from east-north-east to east. Under these conditions, wave measurements in the model showed waves of 1 to 2 feet (prototype) in the eastern end of Salt's Bay, and up to 3 or 4 feet farther west.

5.3 Currents caused by Waves and Tides

Quite a strong littoral current, with speeds up to 3 feet per second, was found to flow westward along that part of the southern shore of Salt's Bay between a point south of the eastern end of the spur wall and Malt's Point. The maximum strength of the current coincided with a combination of wave action and flooding tide with tide levels at high water. The maximum flood of the tide had been found from a field survey to occur at high water, and this field survey also defined the tidal discharge at 26,500 c.f.s. with currents in the main tidal channel near the northern wall of the entrance of 4 to 5 knots. A littoral current towards Malt's Point persisted on the model with ebb as well as flood of the tide, and was associated with a large back-eddy when the tide was ebbing. Wave action alone also produced a westward littoral current. It can be expected that such a drift will also occur with waves from the north-east; and waves from south-east and south, though they have less effect, would not tend to reverse this current.

In the south-eastern corner of Salt's Bay, where wave action is also slight, no currents of major importance were found on the model for waves from east-north-east to east. Based on the goegraphy of the area and the fact that no appreciable waves or currents were found in this area with waves from east-north-east to east, the assumption can be made that erosion of this area is the result of storm (or short-period) waves from the north-east.

5.4 Tests of Measures for Mitigating Erosion

5.41 Area from Eastern End of Spur to Malt's Point

It is first noted that whether any anti-erosion measures are required is a moot point. There is a westward drift, but this may be adequately supplied with sand from the east. A hydrographic survey covering Salt's Bay out to the spur wall would give a definitive answer to the question of whether any changes have occurred in the last ten years. If this is not possible, a survey of high and low water marks along the shore would give a fair indication of shoreline changes. If there has been no change, it can be assumed that a balance has been attained between the rate of sand supply and the drift. If, however, the shore is eroding and it is desired to stop the erosion, or if a wider beach is contemplated, some structural control should be considered.

With this possibility in mind, various structures were installed in the model and tests made of their efficacy in reducing waves and currents likely to cause erosion. Some of the structures showed negligible benefit; submerged breakwaters and dykes running from the landward end of the southern breakwater were in this class. Pile groups offshore decreased wave heights but did not reduce the littoral current. Groynes more or less normal to the beach appeared to be quite effective in retaining drifting sand, and a properly designed groyne field would be a possible solution The solution which appeared on the model to be most satisfactory consisted of raising the existing spur wall above high water, extending it westward to the shore, and eastward for about 200 feet. A wave trap action can be expected to result in the pocket so formed, with shoaling of the area and progradation of the shoreline. The time for the area to fill with sand to the required extent should not be excessive, since the littoral drift caused by the rather fast currents should be appreciable. If more rapid sand accumulation were desired, the drift could be artificially nourished by dumping sand where it could be picked up by the current.

5.42 South-Eastern Corner of Salt's Bay

Erosion in this area, currently active, is presumed to result from north-easterly storms. This condition has not been tested on the model. It would seem that a short dyke running west from the landward end of the southern breakwater could help protect the area from storm damage, as long as rocks of sufficiently large size were

used and the dyke were maintained when required. Alternatively, direct dumping of large sized rocks along the present shoreline could reduce the damage caused by storms.

6. References

Arthur, R.S., Munk, W.H. and Isaacs, J.D. (1952) "The direct construction of wave rays". Trans. A.G.U. Vol. 33, No. 6 Dec. 1952.

Bretschneider C.L. (1958) "Revisions in wave forecasting: deep and shallow water." Proc. Sixth Conference on Coastal Engineering 1958.

Gourlay, M.R. (1964) "Wave Models in the Design of Harbour Works". Inst. of Engineers, Aust. Brisbane Division. Technical Papers Vol. 5 No. 2, Feb. 1964.

Greslou, L. and Mahe, Y. "Etude du coefficient de reflexion d'une houle sur un obstacle constitué par un plan incline." Proc. Fifth Conference on Coastal Engineering, 1954.

Hydrographic Dept. Admiralty, London (1960). "Australia Pilot". Vol. III Fifth Edition 1960, p. 88.

Ippen A.T. and Kulin, G. (1955) "The shoaling and breaking of the solitary wave" Proc. Fifth Conference on Coastal Engineering, 1955.

Mason, M.A. (1951) "The Transformation of waves into shallow water". Proc. First Conference on Coastal Engineering, 1951.

Putnam et al (1949) "Prediction of Longshore Currents" Trans. A.G.U. Vol. 30. No. 3, June 1949.

Savage P.R. (1949) "Laboratory study of the effect of groins on the rate of littoral transport: equipment development and initial tests". Beach Erosion Board Tech. Memo No. 114 Washington 1949.

Sverdrup. H.V. and Munk, W.H. (1946) "Theoretical and empirical relations in forecasting breakers and surf". Trans. A.G.U. Vol. 27-VI.

U.S. Beach Erosion Board (1942) "A Summary of the theory of oscillatory waves". Tech. Report No. 2, 1942.

U. S. Navy Hydrographic Office (1944) "Breakers and surf - principles in forecasting", Nov. 1944.

Weigel R. L. (1961) "Wind Waves and Swell". Proc. Seventh Conference on Coastal Engineering 1961.

APPENDIX I.

Tidal Currents - Prototype Data.

As indicated in Section 3.14, data on tidal velocities in Lake Macquarie Entrance were limited. At the request of the Water Research Laboratory, Hooker-Rex Pty. Ltd. undertook to measure tidal current velocities over a complete tidal cycle at the Swansea Bridge and at 2 sections within the Entrance (shown in Figure 1). The data obtained during this day's work have been reduced to give velocities, and the results are presented in Tables 1, 2 and 3 and Figure 3.

Figure 2 shows the rise and fall of the tide as indicated by a tide gauge which was located on the pier wharf on the upstream side of Swansea Bridge at its southern end, about on the edge of the channel and facing easterly. This location is detailed here as indicating a possible partial explanation of the fact that high tide at Swansea was given by the gauge about an hour earlier than the local ocean high tide, whereas it might be expected to be somewhat later. Information from the Maritime Services Board is that high tide at Swansea Bridge is generally about 1/4 hour later than high tide in the ocean, the latter being close to the time of the high tide at Fort Denison. This estimate is confirmed by the P. W. D. 1954 Hydrographic Survey. The flow of tide past the pier wharf could result in variation of local water level at the gauge with variations in flow, and it may be noted that the time of maximum tidal flow corresponded with the time of high tide registered by the gauge. Another factor that could contribute to local variations in water level would be changes in the wind, although the regularity of the tide curve would suggest that this is not a likely explanation of the discrepancy. On 31.7.64, winds at Nobby's Lighthouse near Newcastle were as given in Table 4, which shows no appreciable weather.

TABLE 4.

WIND AND SEA CONDITIONS AT NOBBYS 31.7.1964.

Time	Wind		Sea
	Direction	Speed-knots	
6 a.m.	N.W.	10	slight low short S.E.
9 a.m.	W.N.W.	10	smooth
12 noon	N.W.	10	"
3 p.m.	N.	5	"
6 p.m.	W.N.W.	10	"
9 p.m.	N.	10	"

APPENDIX I (cont'd.)

Tides registered at Fort Denison were as given in Table 5.

TABLE 5.

TIDES AT FORT DENISON 31.7.64.

Time	Height	
	ft	ins
6.47 am	1	1
1.15 pm	4	4
7.07 pm	1	8

To check whether the tidal flows circulated through the model were producing distributions of current similar to those found in the prototype, current measurements were made on the model with tidal discharges of 0.5 c.f.s. ebb and flood and no waves. Since wave and wind action at the time of the prototype measurements were slight, comparisons between model and prototype will be valid, particularly in regions of appreciable current.

Figures 4 and 5 show the velocities recorded on the model, Figure 3 the velocities measured on the prototype and Figure 6 gives a comparison between the distributions of velocity for model and prototype. Actual values of velocity computed from the model results should not be compared with prototype values, since the tidal discharge was somewhat different, but rather the shapes of the curves. These are seen to be quite similar, the only marked discrepancy occurring during the ebb at the right bank of Section A-A. The model showed an appreciable reverse current, as against the forward current of 1 ft/sec. registered in the prototype. The most probable reason for this would be that the model entry conditions do not produce as wide a spread in the outflow as was found, at least on the date of the measurements, on the prototype. Since conditions during the ebb are not as severe as conditions during the flood, and most of the testing on the model was carried out with inflow, this discrepancy need not be considered serious.

TABLE 1.

Bridge Section.

Stn.	Watch Time	Depth of Lake	Depth of Meter	Velocity ft/sec.	Av. Velocity ft/sec.
1	6.30 am	22'	18'	1.50	1.65
	6.35 am	22'	4'	1.81	
2	6.45 am	25'	20'	2.77	3.23
	6.48 am	25'	5'	3.68	
1	7.38 am	24'	19.5'	1.36	1.42
	7.43 am	24'	5'	1.47	
2	7.53 am	24'	19'	2.24	2.64
	8.03 am	24'	5'	3.04	
1	8.48 am	25'	20'	0.88	0.95
	8.53 am	25'	5'	1.01	
2	9.06 am	25'	20'	1.98	1.97
	9.10 am	25'	5'	1.95	
1	9.52 am	25.5'	no current		
2	10.00 am	25.5'	20'	0.36	0.34
	10.07 am	25.5'	5'	0.32	
1	11.00 am	28'	22.5'	1.47	1.88
	11.05 am	28'	5.5'	2.28	
2	11.12 am	25'	20'	1.29	1.36
		"	5'	1.43	
1	12.12 pm	28.5'	23'	1.90	2.20
	12.17 pm	"	5.5'	2.49	
2	12.24 pm	25'	20'	1.87	1.59
	12.29 pm	"	5'	1.30	
1	1.22 pm	28'	22.5'	1.64	1.90
	1.27 pm	"	5.5'	2.17	
2	1.33 pm	24.5'	19.5'	1.22	1.19
	1.37 pm	"	5'	1.15	
1	2.44 pm	28'	no current		
2	2.55 pm	23.5'	18.5'	no current	
	3.00 pm	"	5'	0.32	0.16
1	3.54 pm	26'	21'	1.08	1.17
	3.59 pm	"	5'	1.26	
2	4.07 pm	23'	18'	1.76	2.25
	4.13 pm	"	5'	2.73	
1	5.12 pm	25'	20'	1.52	1.78
	5.17 pm	"	5'	2.03	
2	5.24 pm	22.5'	18'	2.39	2.66
	5.28 pm	"	4.5'	2.93	
1	6.14 pm	24.5'	19.5'	1.42	1.48
	6.19 pm	"	5'	1.54	
2	6.27 pm	22.5'	18.5'	2.81	2.99
	6.30 pm	"	4.5'	3.17	

TABLE 2.

Section AA.

Stn.	Watch Time	Depth of Lake	Depth of Meter	Velocity ft/sec.	Av. Velocity ft/sec.
1	6.30 am	13'	10.5'	2.67	2.98
	6.33 am	"	2.5'	3.28	
2	6.40 am	3'	2'	1.47	1.47
	6.43 am	"	1'	1.47	
3	6.55 am	4'	3'	0.85	0.88
	7.00 am	"	1'	0.91	
1	8.00 am	16'	13'	1.91	2.36
	8.05 am	"	3'	2.80	
2	8.15 am	5'	4'	0.86	0.93
	8.18 am	"	1'	0.99	
3	8.20 am	5'	4'	0.62	0.67
	8.23 am	"	1'	0.71	
1	9.30 am	18'	14.5'	0.90	1.05
	9.33 am	"	3.5'	1.20	
2	9.40 am	5'	no current		
3	9.50 am	6'	5'	0.25	0.13
		"	1'	no current	
1	10.58 am	18'	14.5'	1.55	1.67
	11.00 am	"	4.5'	1.80	
2	11.06 am	7'	5.5'	0.87	0.98
	11.10 am	"	1.5'	1.08	
3	11.15 am	7'	5.5'	1.22	1.50
	11.18 am	"	1.5'	1.77	
1	12.15 pm	18.5'	15'	1.40	1.66
	12.20 pm	"	3.5'	1.91	
2	12.25 pm	6.5'	5'	1.06	1.14
	12.30 pm	"	1.5'	1.22	
3	12.35 pm	7.5'	6'	1.25	1.35
	12.40 pm	"	1.5'	1.44	
1	1.50 pm	17.5'	14'	1.00	1.07
	1.55 pm	"	3.5'	1.15	
2	2.00 pm	6.5'	5'	0.60	0.65
	2.05 pm	"	1.5'	0.69	
3	2.07 pm	6.5'	5'	0.70	0.77
	2.12 pm	"	1.5'	0.64	
1	3.15 pm	16'	13'	no current	
	3.20 pm	"	3'	0.34	0.17
2	3.25 pm	5.5'	4.5'	0.40	0.44
	3.27 pm	"	1'	0.48	
3	3.32 pm	7'	5.5'	0.48	0.53
	3.40 pm	"	1.5'	0.59	
1	4.40 pm	16'	13'	2.17	2.56
	4.45 pm	"	3'	2.96	
2	4.50 pm	5.5'	4.5'	0.91	1.16
	4.55 pm	"	1'	1.41	
3	5.00 pm	5'	4.5'	0.91	1.04
	5.05 pm	"	1'	1.16	

TABLE 3.

Section BB.

Stn.	Watch Time	Depth of Lake	Depth of Meter	Velocity ft/ sec.	Av. Velocity ft/ sec.
1	7.05 am	7'	5.5'	2.25	2.30
	7.10 am	"	1.5'	2.34	
2	7.15 am	5'	4'	1.39	1.48
	7.22 am	"	1'	1.56	
3	7.25 am	5'	4'	0.76	0.89
	7.30 am	"	1'	1.02	
4	7.36 am	7'	5.5'	no current	
	7.41 am	"	1.5'	0.30	0.15
5	7.50 am	2'		no current	
1	8.33 am	7'	5.5'	1.29	1.32
	8.40 am	"	1.5'	1.35	
2	8.45 am	5.5'	4.5'	0.64	0.77
	8.50 am	"	1'	0.90	
3	8.53 am	6.5'	5.5'	0.37	0.36
	8.56 am	"	1.5'	0.35	
4	9.00 am	7.5'		no current	
5	9.05 am	2'		no current	
1	10.00 am	7'		no current	
2	10.03 am	7'		no current	
3	10.07 am	7'		no current	
4	10.10 am	8'		no current	
5	10.15 am	3'		no current	
1	11.30 am	8.5'	7'	1.26	1.40
	11.35 am	"	1.5'	1.54	
2	11.39 am	7'	5.5'	1.18	1.32
	11.45 am	"	1.5'	1.47	
3	11.50 am	8.5'	6.5'	0.84	0.83
	11.55 am	"	2'	0.83	
4	12.00 noon	9'	7'	0.50	0.54
	12.03 pm	"	2'	0.58	
5	12.06 pm	5'		no current	
1	12.45 pm	8.5'	7'	1.22	1.32
	12.50 pm	"	1.5'	1.41	
2	12.55 pm	7'	5.5'	1.14	1.20
	1.00 pm	"	1.5'	1.26	
3	1.05 pm	8'	6.5'	0.55	~~0.02~~
	1.10 pm	8'	1.5'	0.60	
4	1.15 pm	8.5'	7'	0.41	0.45
	1.20 pm	"	1.5'	0.49	
5	1.25 pm	3.5'		no current	
1	2.18 pm	7.5'	6'	0.70	0.61
	2.22	"	1.5'	0.52	

TABLE 3 (cont'd.)

Section BB.

Stn.	Watch Time	Depth of Lake	Depth of Meter	Velocity ft/ sec.	Av. Velocity ft/ sec.
2	2. 28 pm	6. 5'	5'	0. 51	0. 47
	2. 30 pm	"	1. 5'	0. 44	
3	2. 40 pm	7'		no current	
4	2. 45 pm	8'		no current	
5	2. 50 pm	3'		no current	
1	3. 44 pm	7. 5'	6'	1. 24	1. 48
	3. 48 pm	"	1. 5'	1. 72	
2	3. 52 pm	5. 5'	4. 5'	0. 53	0. 72
	3. 55 pm	"	1'	0. 94	
3	4. 05 pm	6. 5'	5'	0. 39	0. 54
	4. 08 pm	"	1. 5'	0. 70	
4	4. 15 pm	7. 5'	6'	0. 38	0. 36
	4. 20 pm	"	1. 5'	0. 34	
5	4. 25 pm	2'		no current	
1	5. 20 pm	6. 5'	5'	2. 14	2. 24
	5. 25 pm	"	1. 5'	2. 33	
2	5. 30 pm	5'	4'	1. 13	1. 19
	5. 40 pm	"	1'	1. 25	
3	5. 45 pm	6'	4. 5'	0. 64	0. 83
	5. 50 pm	"	1. 5'	1. 02	

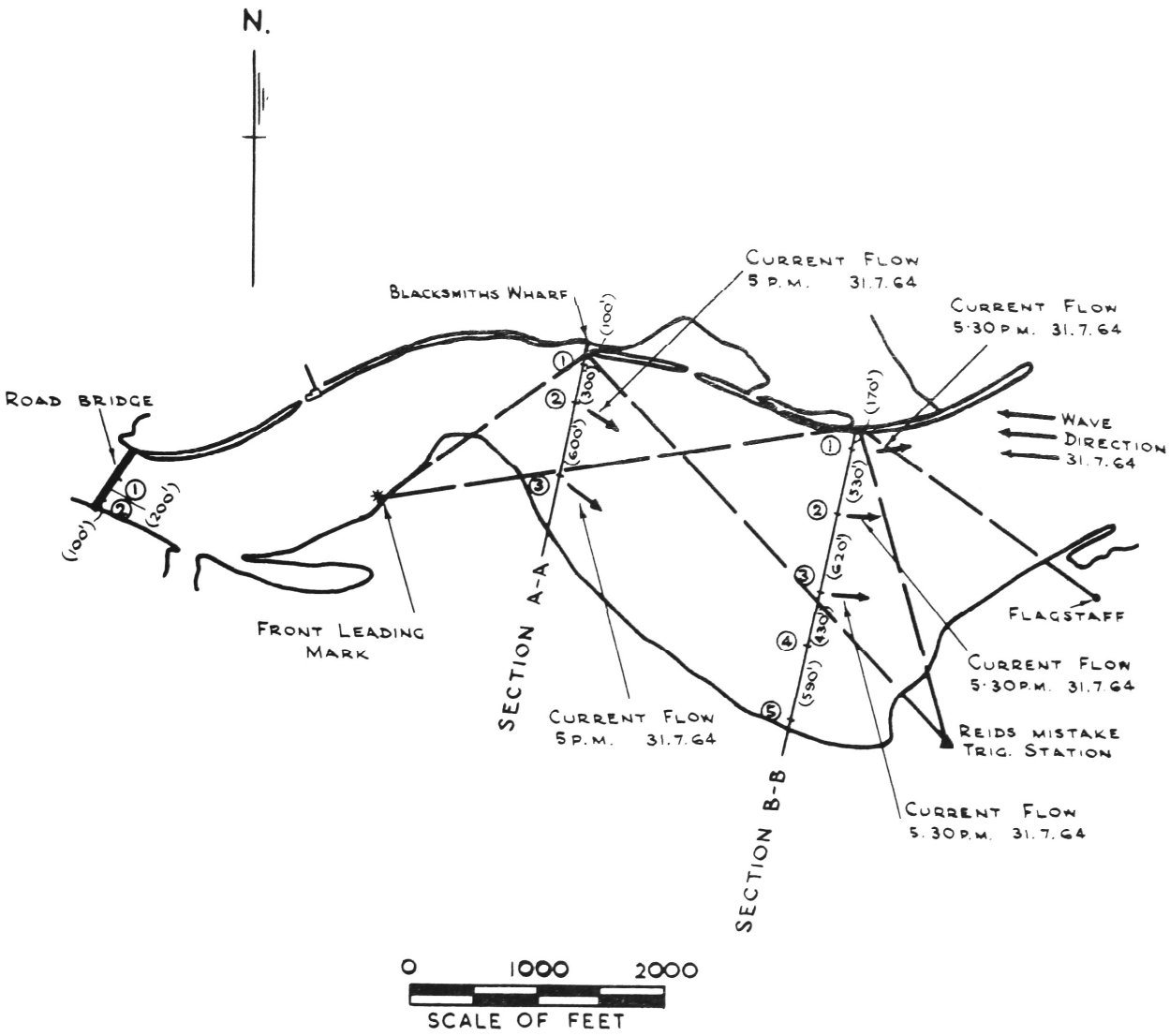

Figure 1: Location of Sections for Velocity Measurements

31.7.1964

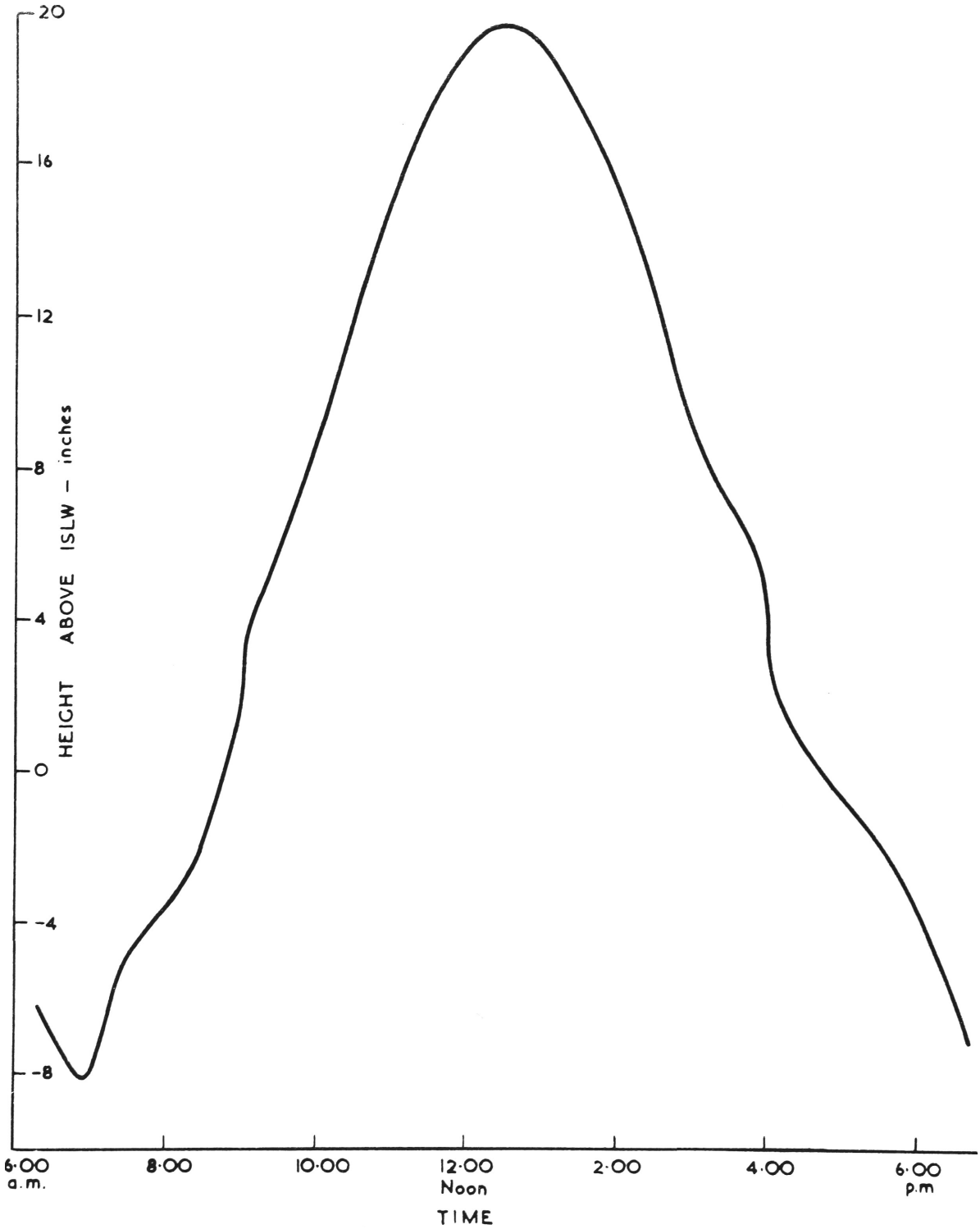

NOTE : Tides at Fort Denison

6·47a.m	0'- 10"
1.15 p.m	4'- 4"
7·07p.m	1'- 6"

Figure 2: Tide Curve for Swansea Bridge. Gauge 31·7·1964

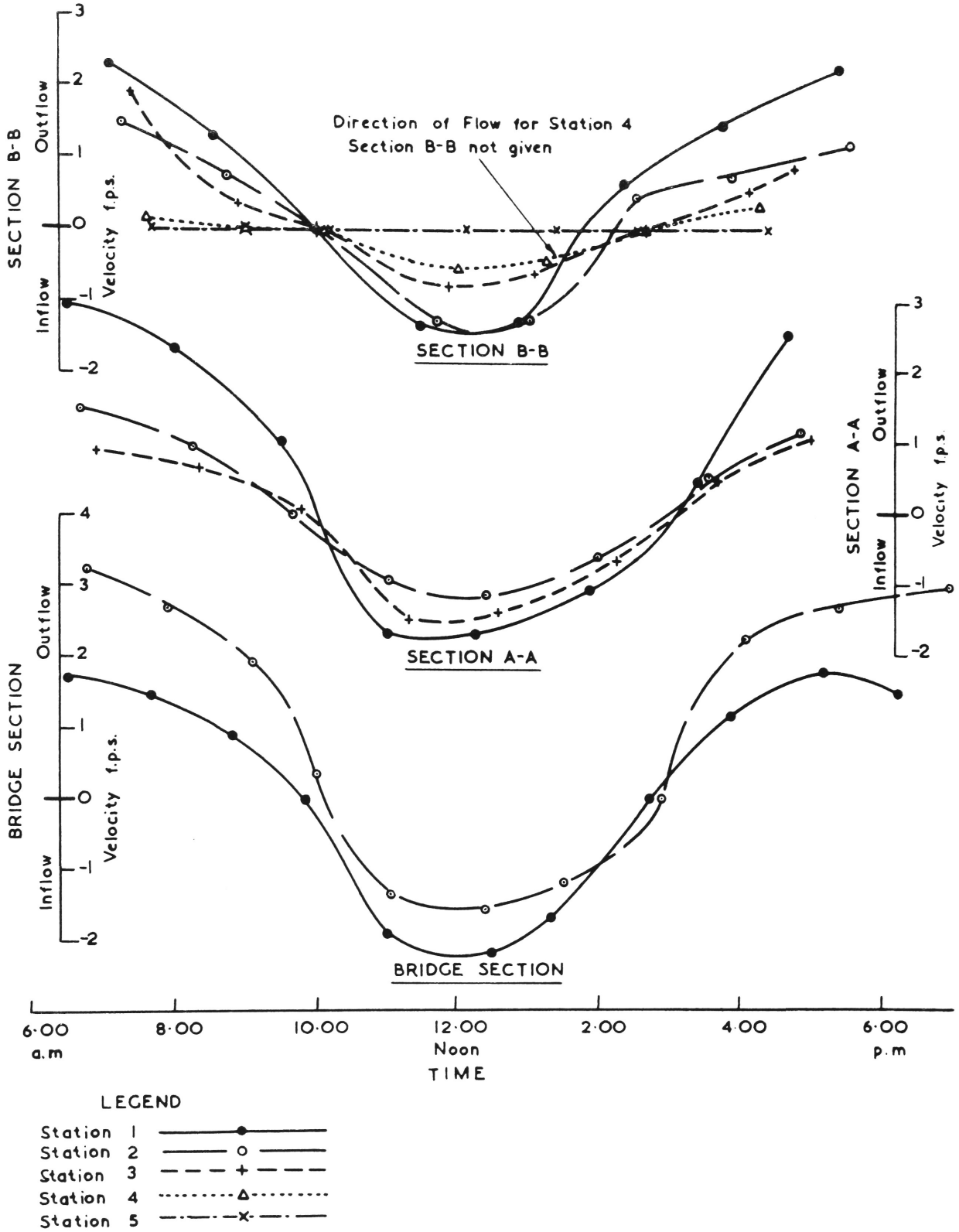

Figure 3: Current Velocities in Lake Macquarie Entrance - 31·7·1964

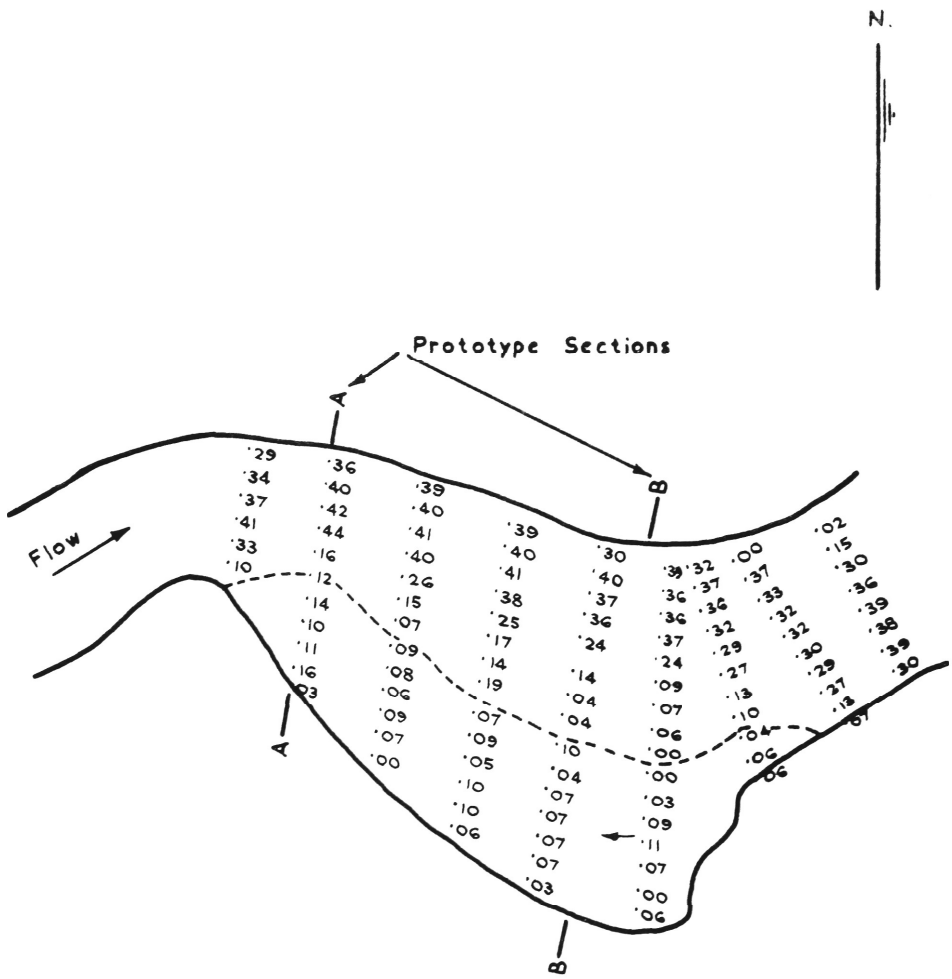

Figure 4: Tidal Current Velocity Measurements

Outflow Q=0·5 c.f.s.

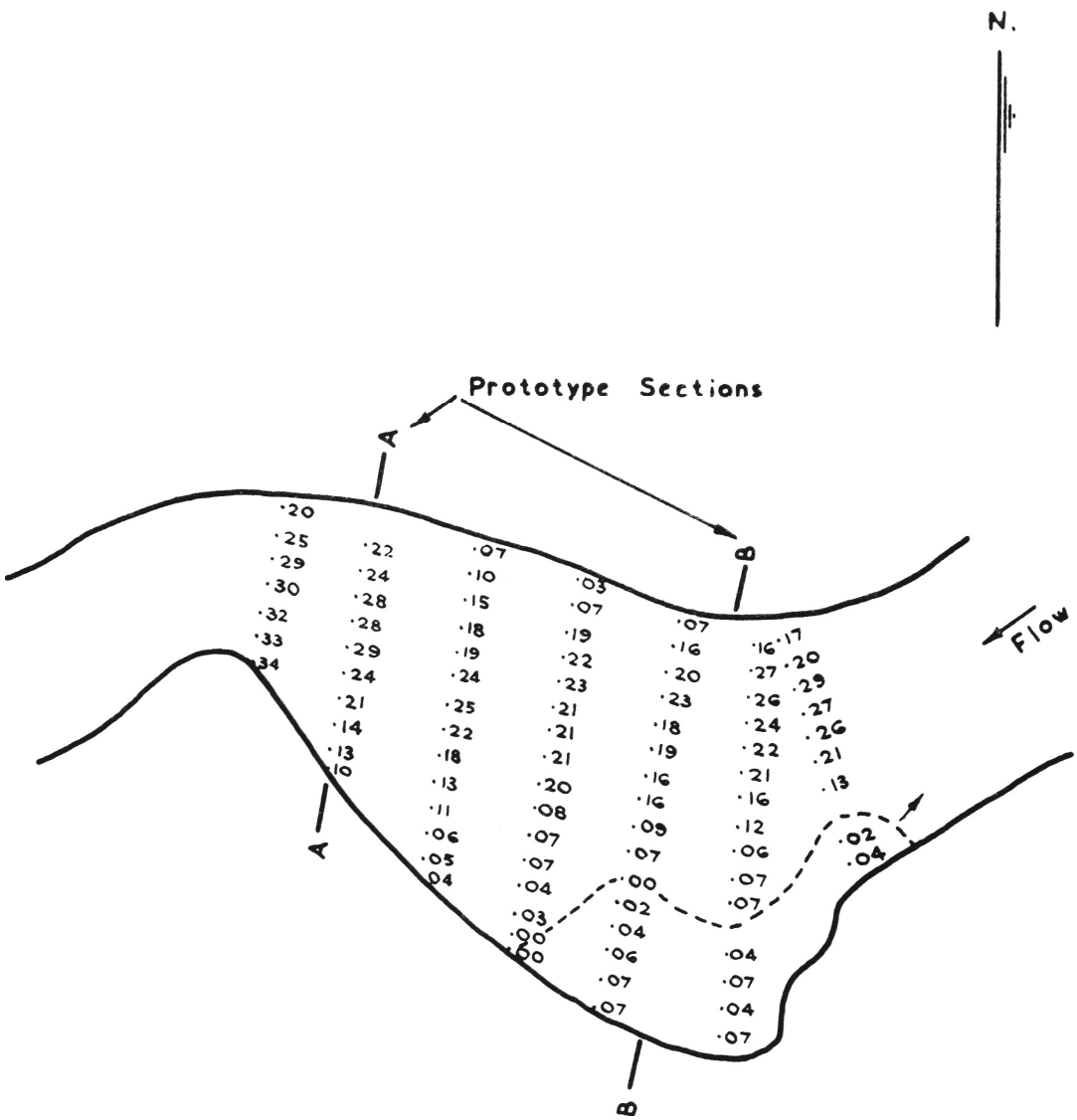

Figure 5: Tidal Current Velocity Measurements

Inflow Q=0·5 c.f.s.

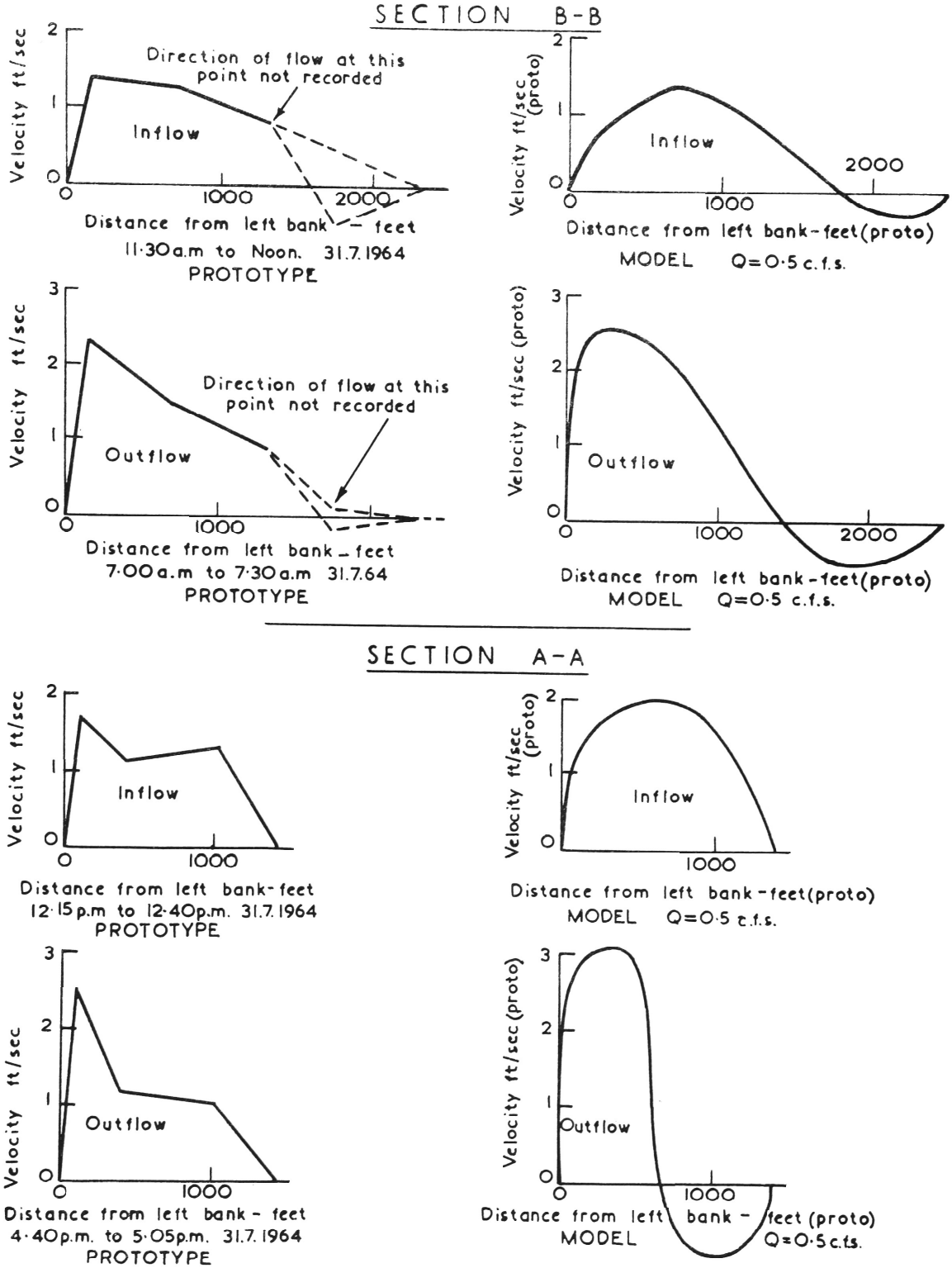

Figure 6: Tidal Current Distributions for Model and Prototype